

## Discovery of alunite in Cross crater, Terra Sirenum, Mars: Evidence for acidic, sulfurous waters <sup>‡</sup>

BETHANY L. EHLMANN<sup>1,2,\*</sup>, GREGG A. SWAYZE<sup>3,\*</sup>, RALPH E. MILLIKEN<sup>4</sup>, JOHN F. MUSTARD<sup>4</sup>,  
ROGER N. CLARK<sup>5</sup>, SCOTT L. MURCHIE<sup>6</sup>, GEORGE N. BREIT<sup>3</sup>, JAMES J. WRAY<sup>7</sup>, BRIGITTE GONDET<sup>8</sup>,  
FRANCOIS POULET<sup>8</sup>, JOHN CARTER<sup>8</sup>, WENDY M. CALVIN<sup>9</sup>, WILLIAM M. BENZEL<sup>3</sup>, AND KIMBERLY D. SEELOS<sup>6</sup>

<sup>1</sup>Division of Geological and Planetary Sciences, California Institute of Technology, Pasadena, California 91125, U.S.A.

<sup>2</sup>Jet Propulsion Laboratory, California Institute of Technology, Pasadena, California 91109, U.S.A.

<sup>3</sup>U.S. Geological Survey, Denver, Colorado 80225, U.S.A.

<sup>4</sup>Department of Earth, Environmental and Planetary Sciences, Brown University, Providence, Rhode Island 02906, U.S.A.

<sup>5</sup>Planetary Science Institute, Tucson, Arizona 85719, U.S.A.

<sup>6</sup>Johns Hopkins University, Applied Physics Laboratory, Laurel, Maryland 20723, U.S.A.

<sup>7</sup>School of Earth and Atmospheric Sciences, Georgia Institute of Technology, Atlanta, Georgia 30332, U.S.A.

<sup>8</sup>Institut d'Astrophysique Spatiale, Université Paris-Sud, Orsay, 91405, France

<sup>9</sup>Department of Geological Sciences, University of Nevada, Reno, Nevada 89557, U.S.A.

### ABSTRACT



Cross crater is a 65 km impact crater, located in the Noachian highlands of the Terra Sirenum region of Mars (30°S, 158°W), which hosts aluminum phyllosilicate deposits first detected by the Observatoire pour la Minéralogie, L'Eau, les Glaces et l'Activité (OMEGA) imaging spectrometer on Mars Express. Using high-resolution data from the Mars Reconnaissance Orbiter, we examine Cross crater's basin-filling sedimentary deposits. Visible/shortwave infrared (VSWIR) spectra from the Compact Reconnaissance Imaging Spectrometer for Mars (CRISM) show absorptions

diagnostic of alunite. Combining spectral data with high-resolution images, we map a large (10 km × 5 km) alunite-bearing deposit in southwest Cross crater, widespread kaolin-bearing sediments with variable amounts of alunite that are layered in <10 m scale beds, and silica- and/or montmorillonite-bearing deposits that occupy topographically lower, heavily fractured units. The secondary minerals are found at elevations ranging from 700 to 1550 m, forming a discontinuous ring along the crater wall beneath darker capping materials. The mineralogy inside Cross crater is different from that of the surrounding terrains and other martian basins, where Fe/Mg-phyllosilicates and Ca/Mg-sulfates are commonly found. Alunite in Cross crater indicates acidic, sulfurous waters at the time of its formation. Waters in Cross crater were likely supplied by regionally upwelling groundwaters as well as through an inlet valley from a small adjacent depression to the east, perhaps occasionally forming a lake or series of shallow playa lakes in the closed basin. Like nearby Columbus crater, Cross crater exhibits evidence for acid sulfate alteration, but the alteration in Cross is more extensive/complete. The large but localized occurrence of alunite suggests a localized, high-volume source of acidic waters or vapors, possibly supplied by sulfurous (H<sub>2</sub>S- and/or SO<sub>2</sub>-bearing) waters in contact with a magmatic source, upwelling steam or fluids through fracture zones. The unique, highly aluminous nature of the Cross crater deposits relative to other martian acid sulfate deposits indicates acid waters, high water throughput during alteration, atypically glassy and/or felsic materials, or a combination of these conditions.

**Keywords:** Alunite, phyllosilicates, hydrothermal activity, lakes, groundwater, Mars, sediments, infrared spectroscopy, Invited Centennial article

### INTRODUCTION

Although geomorphic evidence for the presence of liquid water on Mars has been longstanding (e.g., Carr 1996 and references therein), mineralogic evidence for aqueous alteration of rocks on the martian surface has been revealed relatively recently

by in situ exploration by the Mars Exploration Rovers (MER; e.g., Squyres et al. 2004a, 2004b, 2008; Arvidson et al. 2006) and by high-resolution, orbital infrared spectroscopy. Thermal Emission Spectrometer (TES) data (Christensen et al. 2001), Thermal Emission Imaging System (THEMIS) data (Christensen et al. 2004; Osterloo et al. 2008), and visible/shortwave-infrared (VSWIR) imaging spectrometer data from the Observatoire pour la Minéralogie, L'Eau, les Glaces et l'Activité (OMEGA) on Mars Express (Bibring et al. 2005) and the Compact Reconnaissance Imaging Spectrometer for Mars (CRISM) onboard the Mars

\* These authors contributed equally to this work. E-mail: ehlmann@caltech.edu; gswayze@usgs.gov

Special collection papers can be found online at <http://www.minsocam.org/MSA/AmMin/special-collections.html>

<sup>‡</sup> Open access: Article available to all readers online.

Reconnaissance Orbiter (MRO; Murchie et al. 2007) have revealed sulfates, carbonates, chlorides, phyllosilicates, and other hydrated silicates on the surface of Mars (e.g., Gendrin et al. 2005; Poulet et al. 2005; Bibring et al. 2006; Mustard et al. 2008; Osterloo et al. 2008; Ehlmann et al. 2008; Murchie et al. 2009a). Salts and secondary minerals indicative of water are heterogeneously distributed. Whereas phyllosilicates are widespread and distributed globally in Noachian and some Hesperian terrains, salts such as chlorides, carbonates, and sulfates show more restricted and spatially distinct geographic distributions (e.g., Ehlmann and Edwards 2014). Few hydrated minerals are mapped in Amazonian terrains (e.g., Bibring et al. 2006; Carter et al. 2013). Distinctive martian geochemical environments characterized by different pH, water:rock ratio, and fluid chemistry can thus be inferred. The geologic settings of these salt- and secondary mineral-bearing units vary and include deltaic deposits, basin-filling layered deposits, impact ejecta, and massive units that lack clear bedding.

Here, we report the geologic context and environmental impli-

cations of the first detection on Mars of alunite,  $KAl_3(SO_4)_2(OH)_6$ , using diagnostic shortwave-infrared absorptions in CRISM data (after Swayze et al. 2008). In contrast to calcium and magnesium sulfates, which are the predominant sulfates detected on Mars by orbital and surface data (e.g., Gendrin et al. 2005; Murchie et al. 2009a; Vaniman et al. 2014), alunite is rare and found to date only in the Terra Sirenum region (Swayze et al. 2008; Wray et al. 2011). Alunite is an indicator of distinctly acidic geochemical conditions during precipitation, pointing to low-pH, sulfurous fluids at or near the martian surface. We examine the mineral assemblages, their geomorphology, and regional context to understand the controls on spatially extensive alunite formation in Cross crater and the environmental setting(s) of aqueous alteration.

#### DATA SETS AND METHODS

Cross crater, a 65 km diameter late-Noachian impact crater in the southern highlands of Terra Sirenum (30°S, 158°W; Fig. 1), was targeted by MRO based on an absorption at 2.2  $\mu\text{m}$  seen in a few pixels of OMEGA data, which suggested the presence of an Al-phyllosilicate such as kaolinite (Gondet et al. 2006). Cross crater

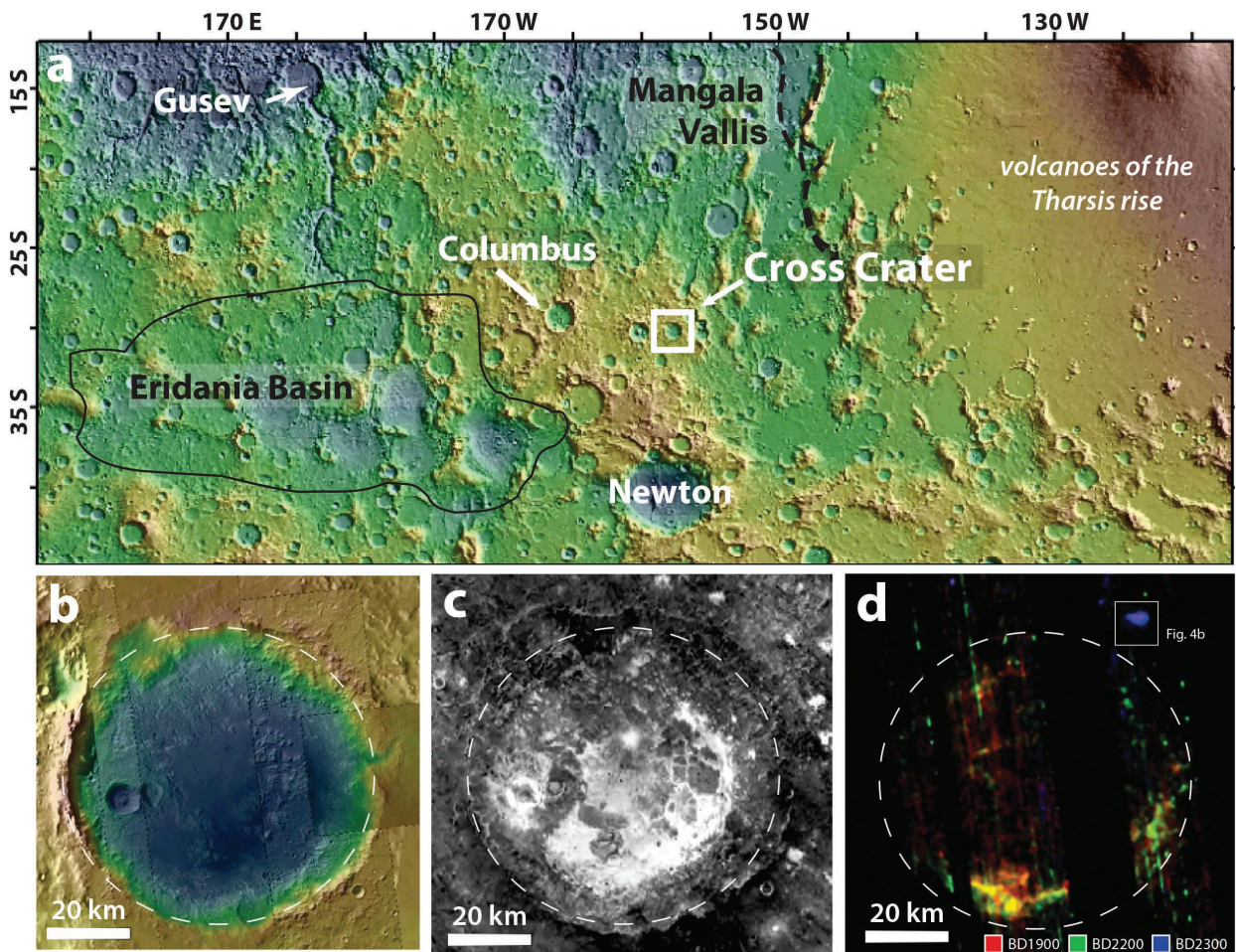


**FIGURE 1.** (a) Location of Cross crater on a MOLA topographic map of Mars where red colors are high elevations and blue are low elevations. Elevation range is approximately  $-2500$  to  $10000$  m. (b) MOLA topographic map of Cross crater overlain on CTX. (c) Nighttime thermal infrared map from THEMIS (Christiansen et al. 2004). Bright-toned areas are warmer and higher thermal inertia. Peak ring materials and bright sedimentary layers are relatively lower thermal inertia relative to a later emplaced dark cap rock. (d) CRISM multispectral maps showing the locations of secondary minerals within and around Cross crater using band depth parameterizations (Pelkey et al. 2007). Red = BD1900 for  $H_2O$  in mineral structures, green = BD2200 for Al-OH and Si-OH, blue = BD2300 for Fe-OH and Mg-OH.

is west of the Tharsis rise volcanic edifice in a faulted area with several candidate closed basin lakes (Anderson et al. 2001; Goudge et al. 2015). Seventeen CRISM images were acquired over Cross crater in 544 spectral channels from 0.4–3.9  $\mu\text{m}$  in full-resolution targeted mode, covering approximately 10 km  $\times$  10 km with a spatial sampling of 18–20 m/pixel, and in half-resolution targeted mode, covering 10 km  $\times$  20 km with a spatial sampling of 35–40 m/pixel (Murchie et al. 2007) (Table 1). In targeted mode, CRISM's effective spectral resolution near 2.2  $\mu\text{m}$  is approximately 10 nm, allowing narrow SWIR absorptions such as the 2.2  $\mu\text{m}$  doublet present in kaolinite group minerals to be resolved. Analyses of data from 0.4–2.6  $\mu\text{m}$  enable identification of minerals using diagnostic electronic absorptions in the visible and shortwave infrared (VSWIR) from transition metals such as iron as well as vibrational absorptions from OH, H<sub>2</sub>O, and CO<sub>2</sub>. Additionally, CRISM data were acquired in multispectral mapping mode over the same wavelength range but with decreased spatial and spectral resolution (Murchie et al. 2007, 2009b). VSWIR remote sensing data measure the composition of the upper hundreds of micrometers of the surface; consequently, determination of the mineralogy of lithologic/stratigraphic units requires the bedrock be at least patchily exposed beneath other surface covers, e.g., dust, sand, or overlying units.

Raw CRISM spectra were processed to I/F (a ratio of measured radiance to incoming solar flux) following the methodology of Murchie et al. (2009b) and were then photometrically and atmospherically corrected using standard procedures. Assuming a surface that scatters isotropically, i.e., a Lambertian surface, scene I/F was divided by the cosine of the incidence angle, and then corrected for atmospheric gas band absorptions by dividing by a scaled atmospheric transmission spectrum (e.g., Mustard et al. 2008; Ehlmann et al. 2009). To highlight spectral features that differ between terrains and to reduce the effect of systematic, detector-dependent instrument artifacts, individual or average spectra from areas of interest were ratioed to an average spectrum of areas located within the same image column and lacking narrow vibrational absorptions. Spectral summary parameters (Pelkey et al. 2007), which spatially map the strength of absorptions related to Fe, OH, and H<sub>2</sub>O at locations diagnostic of minerals and mineral classes were used initially to discover and detect minerals of interest.

The locations of minerals with diagnostic infrared absorptions were also mapped using the Tetracorder spectral shape-matching algorithms and expert system (Clark et al. 2003), coupled with the Clark et al. (2007) spectral library, to create color-coded maps of the distribution of minerals and/or spectral end-members with absorptions in the 1.0–2.6  $\mu\text{m}$  range. Tetracorder compares absorption features in library reference spectra to absorption features in an observed spectrum (e.g., in a CRISM pixel) and then calculates the modified least-squares correlation between them. The algorithm derives a fit (a correlation coefficient) for each of the spectra in its library, applies user-specified constraints on absorption features, and selects the mineral with the highest fit as the best spectral match to the observed spectrum. Maps of the distribution of various minerals are assembled by assigning a unique color to pixels spectrally dominated by a particular mineral or mineral mixture.

CRISM parameter and Tetracorder mineral maps were then map projected and

co-registered with MRO high spatial resolution image data collected at 6 m/pixel by the Context Imager (CTX; Malin et al. 2007) and at 0.3 m/pixel by the High Resolution Imaging Science Experiment (HiRISE; McEwen et al. 2007). HiRISE red-blue anaglyphs and digital elevation models provided high-resolution topographic information at 1 m/pixel for one location where stereo image pairs were available. Topography at larger scales was determined using 128 pixel<sup>o</sup> Mars Orbiter Laser Altimeter (MOLA) global gridded data as well as point shot data acquired with a ~168 m diameter spot-size at ~300 m spacing with an absolute vertical precision of ~38 cm and accuracy of ~1 m (Smith et al. 2001). Additional daytime and nighttime infrared images from THEMIS mosaics provided context for the high-resolution data sets as well as insight into the thermophysical properties of the geologic materials (e.g., Ferguson et al. 2006; Edwards et al. 2011).

## RESULTS

Cross crater hosts a diverse suite of secondary and primary minerals found in discrete geomorphic units. Sedimentary units, mostly restricted to elevations between 700 and 1550 m, contain kaolinite group phyllosilicates and certain locales have alunite, silica and/or montmorillonite, Fe/Mg-phyllosilicates, Fe-oxides, and Fe-sulfates. These units are overlain by unconsolidated sediment (sands) as well as a lithified capping unit with weak SWIR absorptions indicative of pyroxene group minerals. The details of the composition inferred from spectroscopy, the geomorphology, and the distribution of key units are described below.

### Alunite, Al-phyllosilicates, and silica

Three end-member materials have absorptions near 2.2  $\mu\text{m}$ , exhibit consistent and distinctive spectral characteristics (red, blue, green spectra in Fig. 2), display spatial coherence when mapped in CRISM images, and occur in multiple localities in different CRISM images (Fig. 3). Along the southwestern wall, a ~10 km light-toned deposit occurs within a 860–1020 m elevation topographic contour and has a distinctive absorption at 2.17  $\mu\text{m}$ , accompanied by a doublet near 1.4  $\mu\text{m}$  and absorptions at 1.76, 2.32, and 2.52  $\mu\text{m}$ . These absorptions are uniquely characteristic of alunite group minerals [(K,Na,H<sub>2</sub>O)Al<sub>3</sub>(SO<sub>4</sub>)<sub>2</sub>(OH)<sub>6</sub>] (Figs. 2; Hunt et al. 1971; Clark et al. 1990; Swayze 1997; Bishop and Murad 2005). The difference between K-bearing alunite and Na-bearing natroalunite is resolvable at CRISM spectral resolution (Swayze 1997; Bishop and Murad 2005; Swayze et al. 2006, 2014; McCollom et al. 2014). CRISM spectra of the Cross crater deposit have absorptions at 1.43 and 1.48  $\mu\text{m}$ , which are consistent with alunite, whereas natroalunite has longer wavelength absorptions near 1.44 and 1.49  $\mu\text{m}$ , which are not observed. The presence of a 1.9  $\mu\text{m}$  H<sub>2</sub>O combination absorption and the relative weakness and shapes of the ~1.4  $\mu\text{m}$  absorptions may be evidence for a poorly crystalline alunite and incorporation of non-stoichiometric water (e.g., Swayze et al. 2006). Mixtures of well-crystalline alunite with another hydrated phase can also generate these spectral characteristics. Alunite-kaolinite mixtures are observed in other locations at 18 m/pixel observation scale (yellow; Figs. 2 and 3).

The second and most widely occurring end-member with a ~2.2  $\mu\text{m}$  absorption, found in every CRISM image of Cross crater floor sediments are kaolinite group minerals (referred to collectively as kaolins). These have a pronounced asymmetry in their ~2.2  $\mu\text{m}$  absorption, which is due to differences in the relative strengths of the Al-OH doublet absorptions at 2.17 and 2.21  $\mu\text{m}$  (Hunt 1977 and references therein; Clark et al. 1990; Bishop et al. 2008; Swayze et al. 2014). A similar asymmetry in the weaker

**TABLE 1.** CRISM full- and half-resolution images used in this study

CRISM Image ID	Day-of-year	Used in Tetracorder mapping (Fig. 3)
FRT00014744	2009_230	
FRT00011E7D	2009_097	
FRT0000B49F	2008_181	yes
HRL00012386	2009_113	
FRT00019DFE	2010_201	
FRT00021B59	2011_338	
FRT00010AE2	2009_025	
FRT0000D24B	2008_303	yes
FRT00012E09	2009_146	
FRT0000ACE6	2008_136	yes
FRT0000B252	2008_170	yes
FRT0000987B	2008_019	yes
FRT0001EF51*	2011_189	
FRT0001DABB	2011_101	
FRT0001187B	2009_069	
FRT0000CC44	2008_275	yes
FRT000137C2	2009_185	yes

Notes: Images are listed clockwise around the crater, starting at the inflow valley on the east. Coverage is duplicative in some cases. The best images used for Tetracorder mapping (see Data sets and Methods) are indicated. An asterisk on the image ID indicates data that are short wavelength only, i.e., acquired from 0.4–1.0  $\mu\text{m}$  rather than 0.4–4.0  $\mu\text{m}$ . All CRISM images as well as a map of the image footprints are available at the NASA PDS Geosciences Node web site.

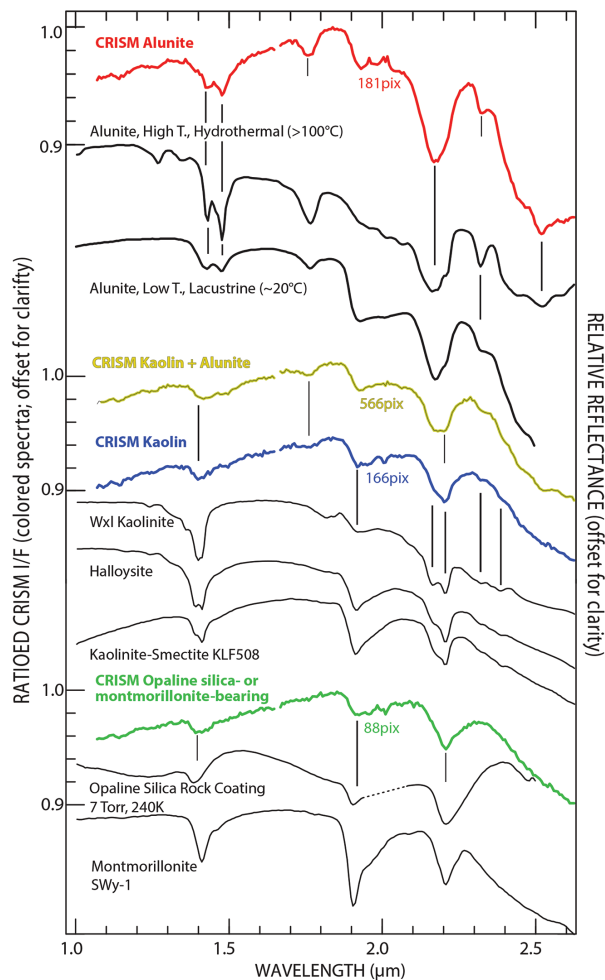


**FIGURE 2.** Spectra of alunite-bearing materials (red), alunite- and kaolin-bearing materials (yellow), kaolin-bearing materials (blue), and silica or Al-smectite-bearing materials (green) from Cross crater CRISM image FRT0000987B compared to library spectra. The low-temperature lacustrine alunite spectrum was acquired of samples from Lake Tyrrell, Australia, and the hydrothermal alunite spectrum was of samples from Marysvale, Utah. The opaline silica acquired under Mars pressure and temperature conditions is from Swayze et al. (2007). All other library spectra are from the Clark et al. (2007) reference database.

1.41  $\mu\text{m}$  absorption due to the Al-OH overtone can also sometimes be resolved. The doublet is not pronounced in the Cross crater materials. As is the case with other kaolin-bearing materials on Mars (e.g., Ehlmann et al. 2009), there is a 1.9  $\mu\text{m}$  absorption due to water that is not typical of well-crystalline, pure kaolinite, but is present in halloysite, mixed-layer kaolinite-smectite clay, impure/disordered kaolinite, or kaolinite physically mixed with hydrated phases. The breadth of the 2.21  $\mu\text{m}$  absorption is also notably wider than end-member spectral library kaolinite group minerals (Fig. 2), indicating the kaolin-bearing phase is likely areally or intimately mixed with other hydroxylated phases, such as montmorillonite, hydrated silica, or alunite at the spatial resolution of CRISM.

The third end-member has a 2.2  $\mu\text{m}$  absorption, also centered

near 2.21  $\mu\text{m}$ , which lacks the asymmetry of kaolinite group minerals and is substantially broader. The center position and lack of a doublet are characteristic of an Al-smectite phase like montmorillonite or an opaline silica phase, with the absorption caused by Al-OH or Si-OH, respectively. The width of the absorption makes opaline silica the most plausible single phase to explain the spectral characteristics; however, mixture of a montmorillonite with opaline silica or another phase, could also cause apparent broadening of the 2.2  $\mu\text{m}$  absorption.

### Iron mineralogy

Fe/Mg-phyllsilicates, the most common phyllsilicate on Mars (e.g., Carter et al. 2013; Ehlmann and Edwards 2014), are uncommon within Cross crater and found so far only in the west, in the vicinity of a small impact crater that excavates Cross crater floor units (Fig. 4). In contrast, multiple localities with Fe/Mg-phyllsilicates are detected in the Noachian plateau unit into which Cross crater was emplaced (e.g., Figs. 1d and 4b). The absorptions due to Fe/Mg-phyllsilicates within Cross crater are centered near 1.43, 1.9, and 2.29  $\mu\text{m}$ , consistent with an Fe-rich smectite such as nontronite (Fig. 4c; Bishop et al. 2002a, 2002b). Outside of Cross crater on the plateau, the terrains have only been observed by CRISM using its multispectral mapping mode, so the spectral resolution for discriminating absorption band minima is lower. However, the composition may be different. Observed absorptions in the Fe/Mg phyllsilicate-bearing terrains near Cross crater are centered near 1.39 and >2.32  $\mu\text{m}$ , which may indicate a different, more Mg-rich, Fe/Mg-phyllsilicate chemical composition.

Within Cross crater and the alunite- and kaolin-bearing materials, CRISM spectra acquired from 0.4–1.0  $\mu\text{m}$  (“S detector data”) exhibit variations in short wavelength spectral slope at 0.4–0.9  $\mu\text{m}$ . These may be due to the presence of iron oxides and/or iron sulfates within the deposits. In CRISM spectral parameters, variation in dust cover is the primary cause of variability in the 0.53  $\mu\text{m}$  band depth parameter rather than crystalline iron oxides; however, certain locations in the sediments and the central ring knobs have absorptions that may indicate a crystalline Fe oxide phase. In image FRT0001187B, there are also several small locations (<250  $\times$  250 m) within the alunite- and kaolin-bearing units with a 0.94  $\mu\text{m}$  absorption. One of these has an atypically sharp absorption at 2.22–2.23  $\mu\text{m}$ , likely an indicator of Fe(III)SO<sub>4</sub>OH, which has been previously detected on Mars in Aram chaos (Lichtenberg et al. 2010) and in opal-bearing, light-toned layered deposits adjacent to Valles Marineris (Miliken et al. 2008). Additionally, knobs that have a yellow-brown tone in CRISM false-color IR images (R: 2.5  $\mu\text{m}$ , G: 1.8  $\mu\text{m}$ , B: 1.2  $\mu\text{m}$ ) have a strong, positive spectral slope downward at wavelengths <1.5  $\mu\text{m}$ , likely caused by one or more Fe-bearing minerals. One small knob in FRT0000987B has spectra consistent with jarosite. A follow-on paper will provide further geologic mapping of all alteration phases, including iron sulfate phases within Cross crater sediments (Swayze et al., in prep.).

Spectral signatures of mafic minerals are uncommon within the crater, found only in overlying sands and certain well-preserved outcrops of caprock. In some locales, the caprock has discernible weak, broad absorptions centered near ~0.9 and ~2.1  $\mu\text{m}$  that are consistent with high-calcium pyroxene group minerals.

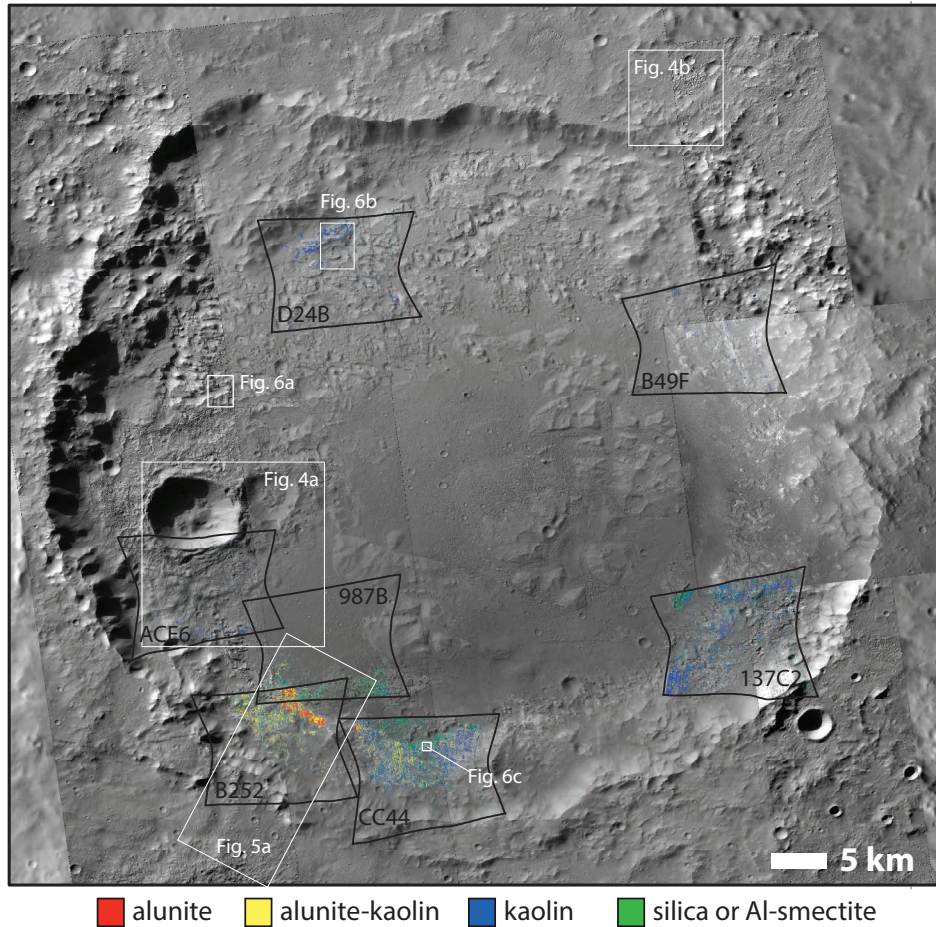


**FIGURE 3.** Tetracorder maps of CRISM images in Cross crater, showing the spatial distribution of the aluminous end-members and their mixtures. Colors correspond to the colors of spectra in Figure 2 and images used in the mapping are listed in Table 1 and indicated here by their image IDs with leading zeros removed.

Olivines and low-calcium pyroxenes are not obviously present, although identification of mafic minerals is complicated by the fact the caprock is the most “bland” material in the scene and thus the typical denominator used to remove residual artifacts. There is variability from place to place in apparent pyroxene content, but the signatures are subtle.

#### Distribution and geomorphology of key intracrater units

The alunite and Al-phyllsilicates are found in sediments ringing the crater floor, typically exposed between a maximum elevation of approximately 1550 m above the MOLA global datum and a minimum elevation of 700 m. Spatial mapping from Tetracorder analyses of CRISM targeted data shows a concentration of pixels most closely matching spectrally dominant alunite along the southwestern crater wall (Fig. 5). Elsewhere, spectral signatures of kaolin-bearing materials are spatially dominant, occurring solely or with variable intermixture of alunite or opaline silica/montmorillonite.

A MOLA point shot profile across the largest spatially contiguous concentration of dominantly alunite-bearing materials shows that the alunite- and kaolin-bearing materials are part

of a bench (Fig. 5b). A break in slope at the transition from the crater wall to the bright-toned sedimentary units suggests that these materials unconformably overlie the crater wall with an upper surface that is nearly horizontal. The alunite is best expressed along the slope, presumably exposed by modern wind erosion (Figs. 5b and 5c). The dominantly alunite portion of the sequence has a lighter-toned, more massive appearance than kaolin-bearing units, and lacks clear bedding, fracturing or other obvious sedimentary structures (Figs. 5d and 5e). The transition from the alunite- and kaolin-bearing materials to the silica/montmorillonite coincides with another break in slope and a change in deposit morphology (position 4 in Figs. 5b and 5c). The alunite- and kaolin-bearing units are massive to layered and form local topographic highs; the silica/montmorillonite-bearing units are polygonally fractured at multiple scales and are topographically lower. The silica/montmorillonite-bearing materials have prominent 500–2000 m long cracks that are tens of meters wide; buttes of dark caprock rest unconformably atop, in some cases straddling these cracks (Fig. 5f). Fracturing in this unit is also common at smaller scales down to a few meters (Fig. 5g).

Al-phyllsilicate-bearing sedimentary units exposed in cross

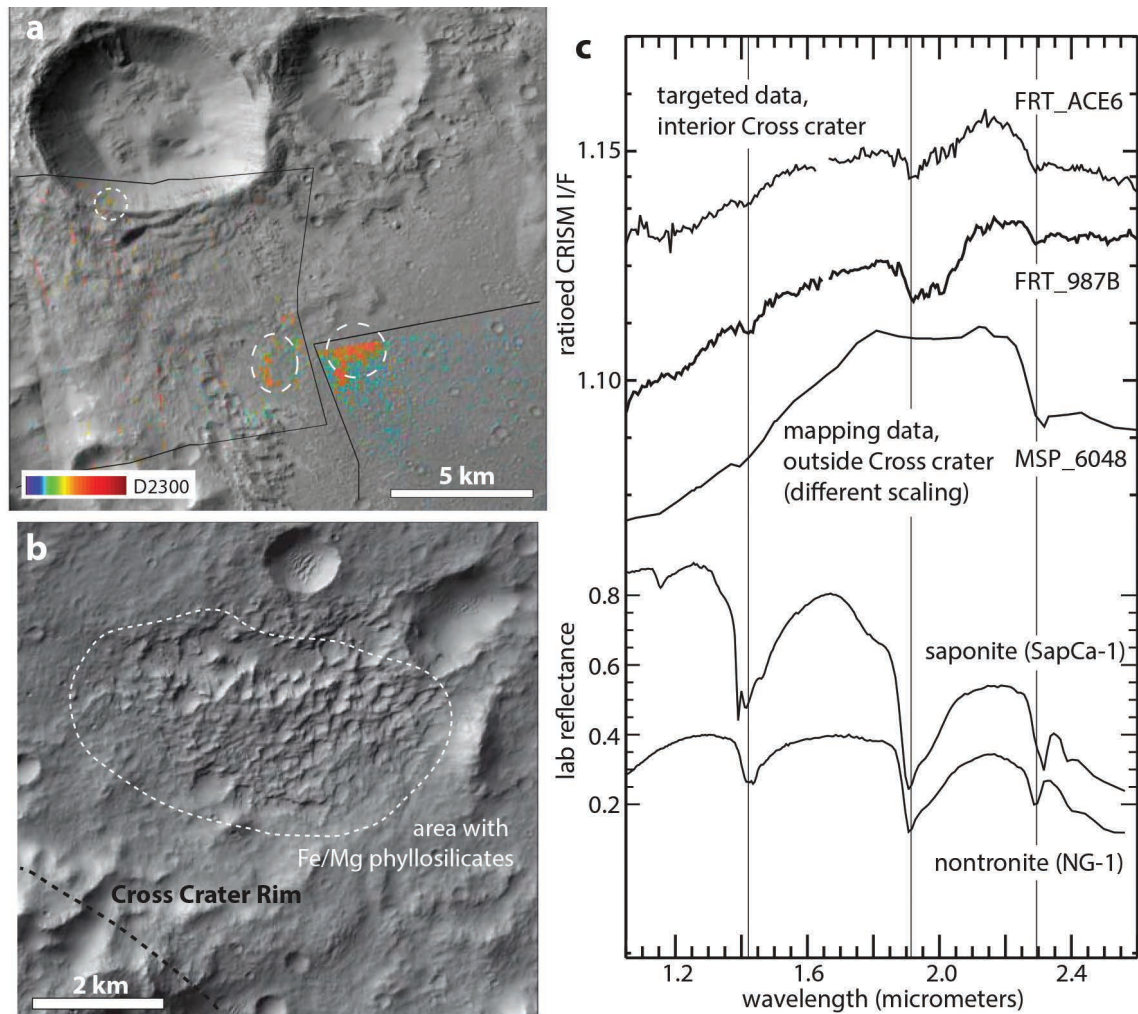


**FIGURE 4.** (a) Fe/Mg-phyllsilicates within Cross crater are found in the rim of a small interior crater as well as at the outer margins of its ejecta blanket. Band depth maps at 2.3  $\mu\text{m}$  from CRISM images FRT0009878 and FRT0000ACE6 were overlain on CTX image P15\_006945\_1494\_XN\_30S158W\_080119 and displayed where values  $>0.0$ . There is some residual striping from detector artifacts in the mineral map. White, circled regions have Fe/Mg-phyllsilicates; spectra are shown in panel c. A context map for the location is in Figure 3. (b) Example of a friable, Fe/Mg phyllosilicate deposit identified in CRISM mapping data shown in CTX image P20\_009028\_1495\_XL\_30S157W\_080629. Spectra from the white, circled area are shown in panel c. A context map for the location is in Figure 1d. (c) Spectra from the locations in a and b compared to laboratory measurements of nontronite, an Fe-smectite, and saponite, a Mg-smectite (Clark et al. 2007).

section are typically layered at a scale of  $<5$  m in thickness (Fig. 6). Buttes of the alunite- and kaolin-bearing remnant layers exist in all sectors of the crater, although coverage of stereo data acquired to date does not yet permit tracing whether bed elevations are continuous across the crater. There are two characteristic types of layering: (1)  $<5$  m thick layers of bright and dark materials exposed on relatively smooth-sloped, continuous scarps (Figs. 6a and 6c) and (2)  $<10$  m thick layers of materials with homogeneous albedo properties but variable erodibility such that they form highly irregular scarps with distinct breaks in slope between layers (Fig. 6b). Type 2 are areally dominant, especially in the northern part of the crater. Type 1 are rarer but are exposed in both the north (Fig. 6a) and in the south (Fig. 6c). Notably, the alunite-bearing materials are not associated with these most clearly layered terrains but rather with units with a

distinctly massive appearance (Fig. 6d).

Overlying the sedimentary materials on the margins of the crater from an elevation of 700–800 m and extending to lower elevations, including the center of the crater, is a darker, rougher looking cap rock unit that lacks a strong spectral signature in CRISM data but has some characteristics indicative of the presence of high-Ca pyroxene group minerals. This dark unit, which is  $<50$  m thick and possibly considerably thinner, may be a coarse-grained sedimentary unit, ash fall, or lava flow. Where removed by erosion, the underlying alunite-, kaolin-, and silica/montmorillonite-bearing units are exposed (Figs. 5e and 5f). Where the dark caprock is preserved, its presence precludes determination of whether underlying aluminous units extend across the entire basin. In addition to being atop the alunite-, kaolin-, and silica/montmorillonite-bearing units, the dark caprock also embays central topographic highs that have

a lower thermal inertia, interpreted to be the peak ring structure of the crater. The dark capping material is brightest in nighttime temperature data (Fig. 1c), suggesting that it is the highest thermal inertia material in the crater, which implies coarser grain size, greater cementation, and/or more coherent bedrock relative to the other units.

The sole intracrater exposure of Fe/Mg-smectites is found

in images FRT0000ACE6 and FRT0000987B, covering an area southeast of a small impact crater, which excavates into caprock and sediments in Cross crater. There is a small area with Fe-smectite in the impact crater's rim in CRISM image FRT0000ACE6 (Figs. 4a and 4c). Additional Fe-smectite deposits are located approximately two crater-radii away from the small impact structure and are slightly higher albedo in the infrared wavelengths than

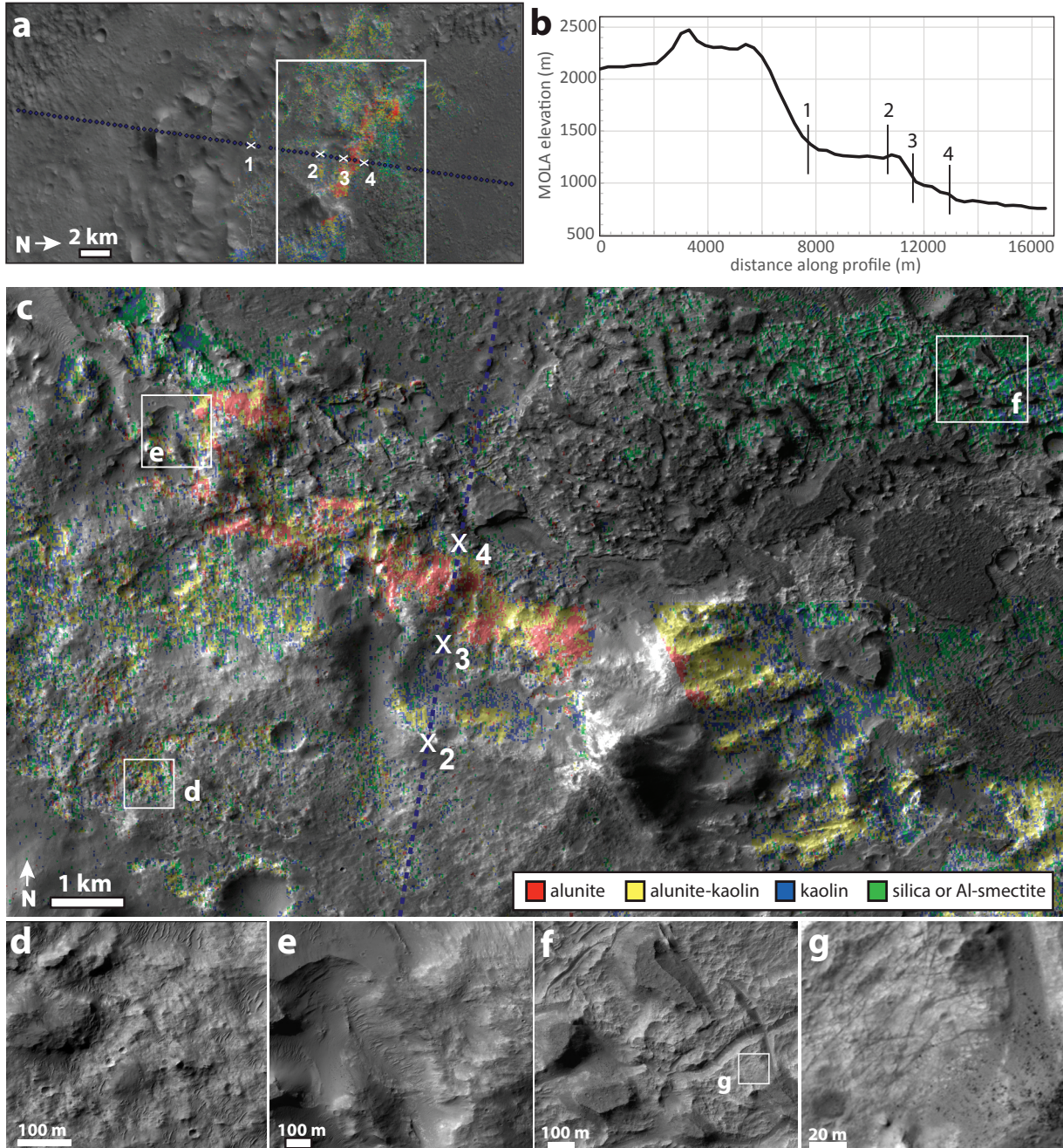


**FIGURE 5.** (a) Context for a MOLA profile of Tetracorder maps on CTX from the southeastern part of Cross crater. The white box shows a portion of c. (b) MOLA point shot data show the alunite/kaolinite-bearing units form a distinctive bench with topographically lower silica or montmorillonite deposits. (c) Tetracorder maps on CTX from the southwestern part of Cross crater showing the morphology of mineral-bearing units. (d and e) Alunite units are massive beneath dark materials in HiRISE PSP\_008883\_1490\_RED. Silica-bearing units are fractured at (f) kilometer scale and (g) meter scale in HiRISE ESP\_016320\_1490\_RED. The silica-bearing materials occur beneath a dark cap rock.

surroundings. Indistinctly layered materials in the upper part of the stratigraphy are the likely host materials. There are some linear features radial to the crater, indicating the presence of ejecta streamers; however, the majority of the small crater's rim rock and ejecta do not have Fe/Mg-phylosilicate signatures. Consequently, it is not clear if the Fe-smectites are in the ejecta or in underlying materials scoured and exposed by the ejecta. FRT00012E09 also may have spectra of Fe/Mg-smectites in a window beneath the caprock, although the signature is weak, restricted to <10 pixels; and CTX resolution is insufficient to resolve the morphology. Resolving the morphology and stratigraphy of the Fe/Mg phyllosilicates in Cross crater will have to await acquisition of further CRISM and HiRISE data in and around the small crater.

### Mineralogy and geomorphology of the Cross crater region

The mineralogy immediately outside of Cross crater is substantially different from that of within (Fig. 1d). No Al-phylosilicates or sulfates are found; but in a survey of the multispectral data within several Cross crater radii, there are at least a half dozen small (~10 km<sup>2</sup>) exposures of Fe/Mg-phylosilicate-bearing materials. Fe/Mg-phylosilicates are found in several apparently sedimentary deposits as well as in small crater ejecta north of Cross crater. These occurrences are associated with high-thermal inertia materials (e.g., Figs. 1c and 1d) yet have a friable, eroded appearance (Fig. 4b). To the south Fe/Mg-phylosilicates are found together with chlorides in a high-thermal inertia deposit near 32°S, 157°W (see Osterloo et al. 2010; Fig. 13d in Ruesch et al. 2012).

Gridded MOLA DEM data of Cross crater paired with visible images show a ~4 km wide valley that breaches the eastern crater rim, entering the Cross crater basin (Fig. 7). No outflow is apparent, and thus Cross crater is a closed basin. The valley enters the crater at an elevation of 1650 m—slightly above the 1550 m maximum height of the alunite and Al-phylosilicate units—from the topographic depression immediately east of the crater. The depression's present extent is ~100 km<sup>2</sup>, although its topography has been modified by a nearby impact crater to the east, so the extent may have previously been greater. Interestingly, small knobs in the walls of the inlet exhibit similar composition to the Cross crater sediments with aluminous (Al-OH bearing) materials. Four knobs in the valley wall have an absorption at 2.18–2.20 μm in materials that also sometimes have a 1.9 μm absorption (Figs. 7d–7g). Analysis of HiRISE and CTX imagery shows that these knobs are part of the walls of the valley, rather than ejecta or debris from the plateau above and are not layered. They occur at an elevation of ~2000 m, i.e., ~400–500 m above the highest outcrops of alunite and Al-phylosilicates minerals within layered Cross crater sediments.

## DISCUSSION

### The Cross crater mineral assemblage in a martian context

Several intercrater depressions across Mars host chlorides or sulfates (Osterloo et al. 2010; Gaillard et al. 2013; Ehlmann and Edwards 2014). Carbonates have only been identified in two potential lake basins (Ehlmann et al. 2009; Michalski et al. 2013). Only a few dozen of the >200 potential closed-basin crater lakes on Mars exhibit evidence of hydrated minerals in

existing CRISM and OMEGA data (Goudge et al. 2015). In deep basins filled with sediments (comparable in size and original depth to Cross crater), sulfates are typically the salt present, associated with Fe/Mg-phylosilicates, hematite, and silica [e.g., in Gale (Milliken et al. 2010) and Terby craters (Ansan et al. 2011)]. Meridiani Planum, explored by the Opportunity rover, has jarosite within its spatially extensive sulfate-rich sediments (Klingelhöfer et al. 2004; Arvidson et al. 2006; Poulet et al. 2008). The Valles Marineris troughs and associated chaos terrain also host sulfates, with some exposures including interbedded or overlying detrital phyllosilicates or authigenic hydrated silicates (e.g., Gendrin et al. 2005; Murchie et al. 2009a; Bishop et al. 2009; Lichtenberg et al. 2010; Roach et al. 2010; Thollot et al. 2012). Typical Valles Marineris interior layered deposit mineralogy is of monohydrated Mg-sulfates interbedded with or grading up-section into polyhydrated sulfates, both accompanied by crystalline ferric oxides (Bibring et al. 2007; Murchie et al. 2009c). Some locales host evidence for distinctly acidic conditions and sulfur-rich fluids. These include Gusev crater (Hurowitz and McLennan 2007; Morris et al. 2008; Wang et al. 2008); jarosite in some units at Northeastern Syrtis Major (Ehlmann and Mustard 2012) and Mawrth Vallis (Farrand et al. 2009, 2014); Valles Marineris plateau deposits with jarosite and Fe(III)SO<sub>4</sub>OH (Milliken et al. 2008; Weitz et al. 2010); jarosite in Noctis Labyrinthus troughs (Thollot et al. 2012); szmolnokite and Fe(III)SO<sub>4</sub>OH low in the section in Aram chaos (Massé et al. 2008; Lichtenberg et al. 2010); and chasma deposits whose spectra exhibit a “doublet” absorption that may be indicative of clays that have been leached or mixed with jarosite (Roach et al. 2010; Weitz et al. 2011). Alunite has not yet been detected in or around any of these regions.

Cross crater contains the first and, as of this writing, largest discovery of alunite deposits on Mars. The outcrop with spectrally dominant alunite in the southwestern portion of the crater is ~10 km × ~5 km in extent, and scattered smaller outcrops occur in several locations in Cross crater, intermixed with kaolinite group minerals. On Mars, known occurrences of alunite are so far restricted to three locations in the Terra Sirenum region: (1) Cross crater; (2) nearby Columbus crater, where it is found mixed with phyllosilicates in CRISM image, FRT00013EEF, in a few hectometer-scale outcrops on the crater lower wall and floor; and (3) a small light-toned deposit within the intercrater plateau near Cross and Columbus (25.42°S, 161.17°W). As described by Wray et al. (2011), Columbus crater has light-toned layered deposits similar in morphology to some within Cross crater (Figs. 6a and 6c) with secondary minerals and precipitates dominated by kaolinite and polyhydrated and monohydrated Ca/Mg/Fe-sulfates, including gypsum and kieserite. Localized outcrops within Columbus contain Al-smectite clays, Fe/Mg-phylosilicates, jarosite, alunite, and crystalline ferric oxides. The interbedded kaolinite and sulfates at Columbus are inferred to represent fluctuating lake levels within a deep, closed-basin deep lake, fed by upwelling groundwaters (Wray et al. 2011). This mineral assemblage is, however, distinct from that in Cross crater.

### Inferred Cross crater water chemistry

At Cross crater, Al-rich and Si-rich phases—specifically, alunite, kaolinite group phyllosilicates, and silica or montmo-

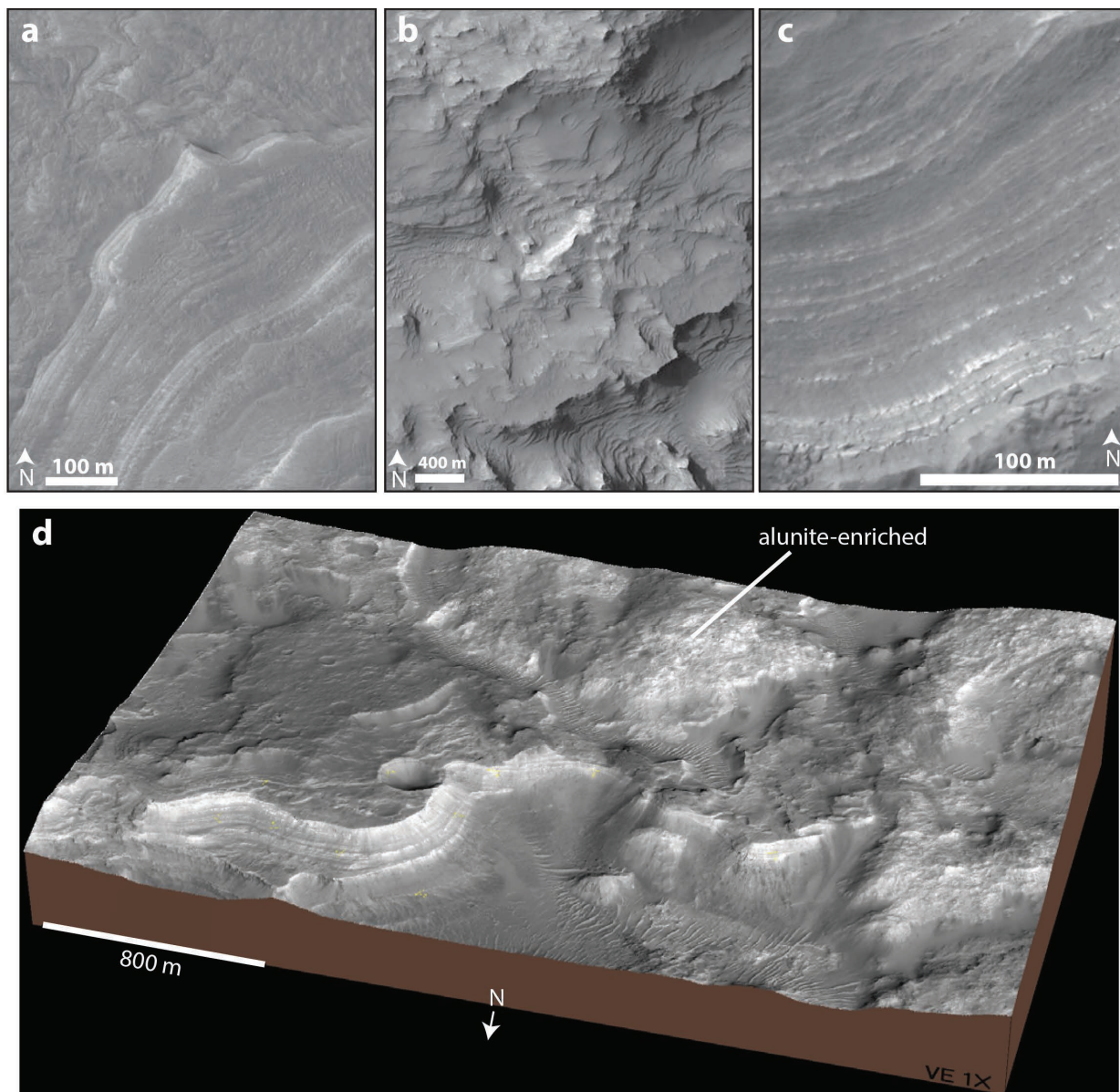


**FIGURE 6.** Finely layered Al-phylosilicate-bearing Cross crater sedimentary materials in (a) northwestern Cross crater in ESP\_013274\_1495\_RED, (b) northern Cross crater in PSP\_010584\_1500\_RED, and (c) southern Cross crater in PSP\_010228\_1490\_RED. Eroded Cross crater sediments have two characteristic types of layering, typified, respectively, by a and c and the more spatially widespread b. (d) A 3D perspective view of the southern wall of Cross crater shows the eroded topography and how the most alunite-enriched area has a distinct lack of bedding. HiRISE digital elevation model from PSP\_010228\_1490 and ESP\_016320\_1490.

rillonite—are the spectrally and spatially dominant secondary minerals. Iron oxides and iron sulfates are also present but are less spatially widespread at the surface. On Earth, this mineral assemblage is classically characteristic of acid sulfate, advanced argillic alteration. As pH decreases, the solubility of  $\text{Al}^{3+}$  increases, making it a mobile element and readily available for incorporation into precipitated secondary minerals. The pH of waters implied by the presence of alunite is acidic and possibly as low as 2–3. Figure 8 presents mineral stability fields for select slices of the multi-dimensional geochemical parameter space that illustrate key tradeoffs in predominance of alunite with other minerals.

Under conditions where  $\text{Al}^{3+}$  is enriched in fluids, kaolinite and alunite precipitate under similar conditions but with alunite forming at lower pH and/or higher  $a_{\text{SO}_4}$  than kaolinite (Fig. 8a). The formation of alunite also requires acid sulfate solutions that can mobilize potassium in addition to the aluminum (Rye et al. 1992). Aluminum must be many times more concentrated than iron in solution for alunite formation to be favored relative to jarosite formation (Fig. 8b). Jarosite precipitation also requires more oxidizing conditions than alunite precipitation (Fig. 8c). Alunite forms near the  $\text{H}_2\text{S}-\text{SO}_2$  buffer at low  $f_{\text{O}_2}$ , commonly in the near-subsurface (Rye et al. 1992; Stoffregen et al. 2000).

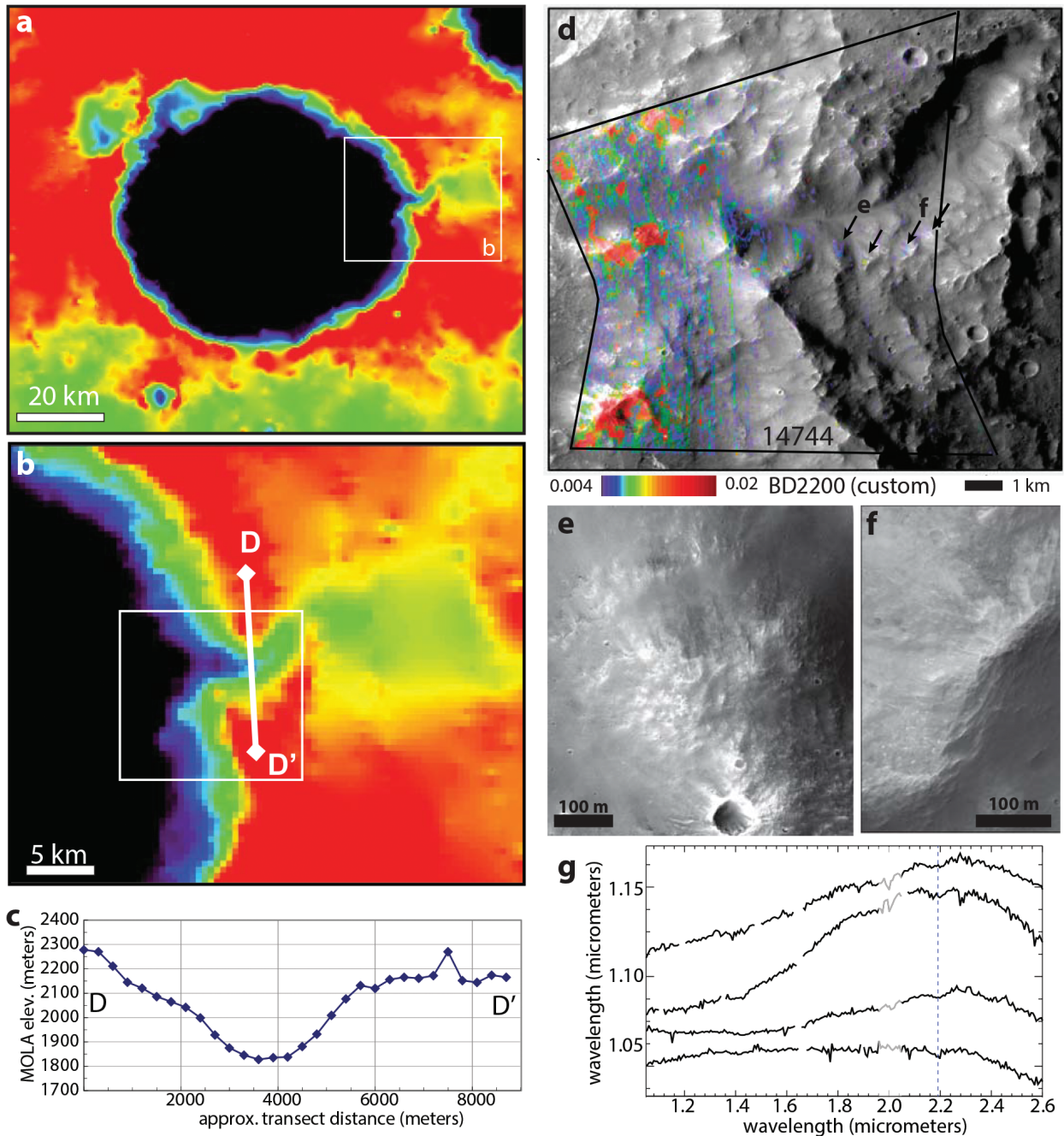


**FIGURE 7.** (a) MOLA topographic image of Cross crater with color gradient across the topographic range subset to emphasize topography in the vicinity of Cross crater. The range shown is from approximately 600 to 2600 m above the MOLA datum. (b) Zoom of a showing the eastern inlet valley and a putative inlet valley into Cross crater. (c) Topographic profile across the valley. (d) A CRISM mineral map tracking the depth of an absorption near 2.17–2.20  $\mu\text{m}$ . The strongest signatures are within Cross crater in sediments. Four locations along the inlet valley, 200 m higher in elevation, also exhibit absorptions characteristic of aluminous materials. HiRISE images from (e) ESP\_012641\_1495\_RED and (f) ESP\_033383\_1495\_RED show the outcrops of materials in the valley at finer spatial resolution. (g) CRISM spectra from FRT00014744 at the four locations.

The coexistence of alunite, kaolinite group phyllosilicates, and silica or montmorillonite may indicate temporally fluctuating pH conditions in waters whereby at low  $a\text{SO}_4^{2-}$ , kaolinite is favored, whereas at lower pHs and/or higher sulfate contents, alunite preferentially precipitates (Fig. 8). Alternatively, a

two-step formation process is possible. From preexisting Al-phyllosilicates, alunite forms by their leaching with waters with sulfuric acid (e.g., Altheide et al. 2010). In either case, Cross crater hosted distinctly sulfurous, acidic waters during at least one part of its history. Determining the timing and environmental

setting(s) of alunite and Al phyllosilicate formation requires additional information, discussed below.

### Possible formation environments for large alunite deposits

How could such a large-scale alunite-bearing deposit form on Mars in Cross crater? On Earth, there are three main environmental settings of alunite precipitation: magmatic hydrothermal systems, weathering of massive sulfide deposits (supergene alteration), and in cratonic lakes fed by paleobrines. On Mars, there are at least four possibilities. For the first possibility, in magmatic hydrothermal systems,  $H_2S$  or  $SO_2$  gases interact with groundwaters, which are then piped to the surface as brines or steam, often along structurally controlled faults (e.g., John et al. 2008; Varekamp et al. 2009). For example, at Copahue volcano in the Andes, argillaceous deposits along the crater lake and flanks of the volcano host alunite and kaolinite in varying proportions, fed by groundwaters whose flow patterns are controlled by faults. Accessory silica phases are interspersed as crusts and veins, and almost pure siliceous sinters occur in zones with low pH. In this and other fumarolic systems, magmatic fluids contribute  $SO_2$  that undergoes disproportionation as it cools to form highly acidic fluids, which boil at the surface of a water table releasing  $H_2S$ - and  $H_2SO_4$ -rich steam that leaches overlying rocks replacing them with alunite and silica (Rye et al. 1992). Lake margins deposits can also contain jarosite, hematite, montmorillonite, gypsum, kaolinite, goethite, and quartz; vent mouths have sulfur and pyrite (Mas et al. 1996). The primary controls on mineralogy are pH,  $f_{O_2}$ , and presence of sulfurous species. Variability is driven by volcanic activity (the vigor of outgassing) and seasonal fluxes, which dictate the relative proportion of meteoric waters to magmatic groundwaters. The fluids containing  $H_2SO_4$ ,  $SO_2$ , HF, and HCl acquire many rock-forming elements from interaction with basaltic to basaltic-andesite protoliths but are not fully neutralized by the interaction (Mas et al. 1996; Varekamp et al. 2009). Upon loss of S, either via decreased production of volcanic steam or reaction with host rocks, sulfurous brines transition to alkaline chloride fluids (Rye et al. 1992). On Mars, acid hydrothermal systems have been proposed for sulfate and silica deposits observed by the Spirit Rover in Gusev crater (e.g., Squyres et al. 2008; Wang et al. 2008) and sulfate deposits in Valles Marineris (e.g., Thollot et al. 2012).

A second possibility is the formation of acidic waters, and then alunite deposition, driven by acidity produced during oxidative weathering of ferrous minerals, like sulfides and primary mafic phases. Such processes typically result in the precipitation of Fe-rich minerals, including ferrous and ferric sulfates as well as iron oxides and phyllosilicates (e.g., Fernández-Remolar et al. 2003, 2005, 2011; Swayze et al. 2000, 2008). The oxidation and hydrolysis of iron from sulfides releases  $H^+$  and is the source of acidity, which dictates the water chemistry and drives subsequent reactions. In these settings, kaolinite and alunite can sometimes be present when altered rocks are felsic or when leaching is intense. Evidence for large quantities of buried sulfides have not been found on Mars, though sulfide weathering has been proposed to explain sulfate deposits (Poulet et al. 2008; Dehouck et al. 2012), and a similar mechanism of near-surface oxidation of Fe(II)-bearing sulfurous groundwaters has been proposed to generate the acid conditions recorded at Meridiani Planum (Hurowitz et al. 2010).

A third possibility is that Cross crater was a paleolake, analogous to the acid saline lakes of Western Australia (WA; e.g., Long et al. 1992; McArthur et al. 1991; Bowen and Benison 2009; Story et al. 2010). The WA lakes do not evolve from evapoconcentration of dilute inflow waters but instead are fed by highly evolved, regionally acid-saline groundwaters. Lakes precipitate halite, gypsum, hematite, kaolinite, and small amounts of basaluminite, bassanite, and alunite. Shallow groundwaters in adjacent mudflats precipitate the same minerals, plus jarosite, which forms syndepositionally as cements and displacive crystals (Benison et al. 2007; Story et al. 2010; Bowen et al. 2012; Benison and Bowen 2015). Alunite is an early diagenetic precipitate within the pores of these deposits. Mixing in of meteoric waters, marine aerosols, evapoconcentration, and mineral precipitation and dilution reactions control the chemistries of individual lakes as well as their time variation. While several theories have been put forward for understanding the origin of the acid saline waters, neither lithologic control (e.g., mafic vs. felsic or presence/absence of massive sulfide), trapped ancient seawaters, or anthropogenic activities can fully explain the observed chemical variability. The lack of natural buffers in a stable, highly weathered craton, coupled with aridity to prevent dilution, may allow ancient acidic brines that have evolved past the carbonate geochemical divide, consuming alkalinity, to acquire acidity from small amounts of Fe, S, and rock weathering (Long et al. 1992; Bowen et al. 2012; Benison and Bowen 2015). Whether such multigeneration brines—or the equivalent of a weathered craton—exist buried in the Mars subsurface is unknown, though production of subsurface brines from dissolution of ancient salt deposits has been hypothesized (Zolotov and Mironenko 2014).

A fourth possibility may be distinctly martian: highly acidified snows/rains. A straightforward way to produce the requisite  $H_2SO_4$ -bearing solutions for alunite formation is via disproportionation of  $SO_2$  released by volcanism into the atmosphere, and subsequent aerosol deposition (Bullock and Moore 2007). Any waters—precipitation and/or snow/ice melt—would become acidic by the incorporation of these hydrous sulfate species, present in the atmosphere but also in the martian soils where there is an imbalance with more anion species than cations (Settle 1979). These acidified waters could episodically form ponds in Cross crater and in surrounding depressions.

### Environment of alunite formation in Cross crater

Geologic associations of minerals present can be used to discriminate between the four possibilities above to establish environmental conditions for the formation of Cross crater's deposits. Most open- and closed-basin lakes on Mars with evidence for secondary minerals exhibit phyllosilicates within the basins that are spectrally identical to materials in the nearby watershed, suggesting transport and deposition may be responsible for the current distribution of these minerals, rather than in situ precipitation (Goudge et al. 2012a, 2015). In Cross crater, however, phyllosilicate mineralization likely occurred in situ because kaolin-bearing sediments within the basin differ markedly from Fe/Mg-phyllosilicates present in plains outside the crater. The existence of extensive kaolinite group minerals and alunite within the basin points to a special geologic process or a peculiar sediment or water chemistry uniquely confined to the

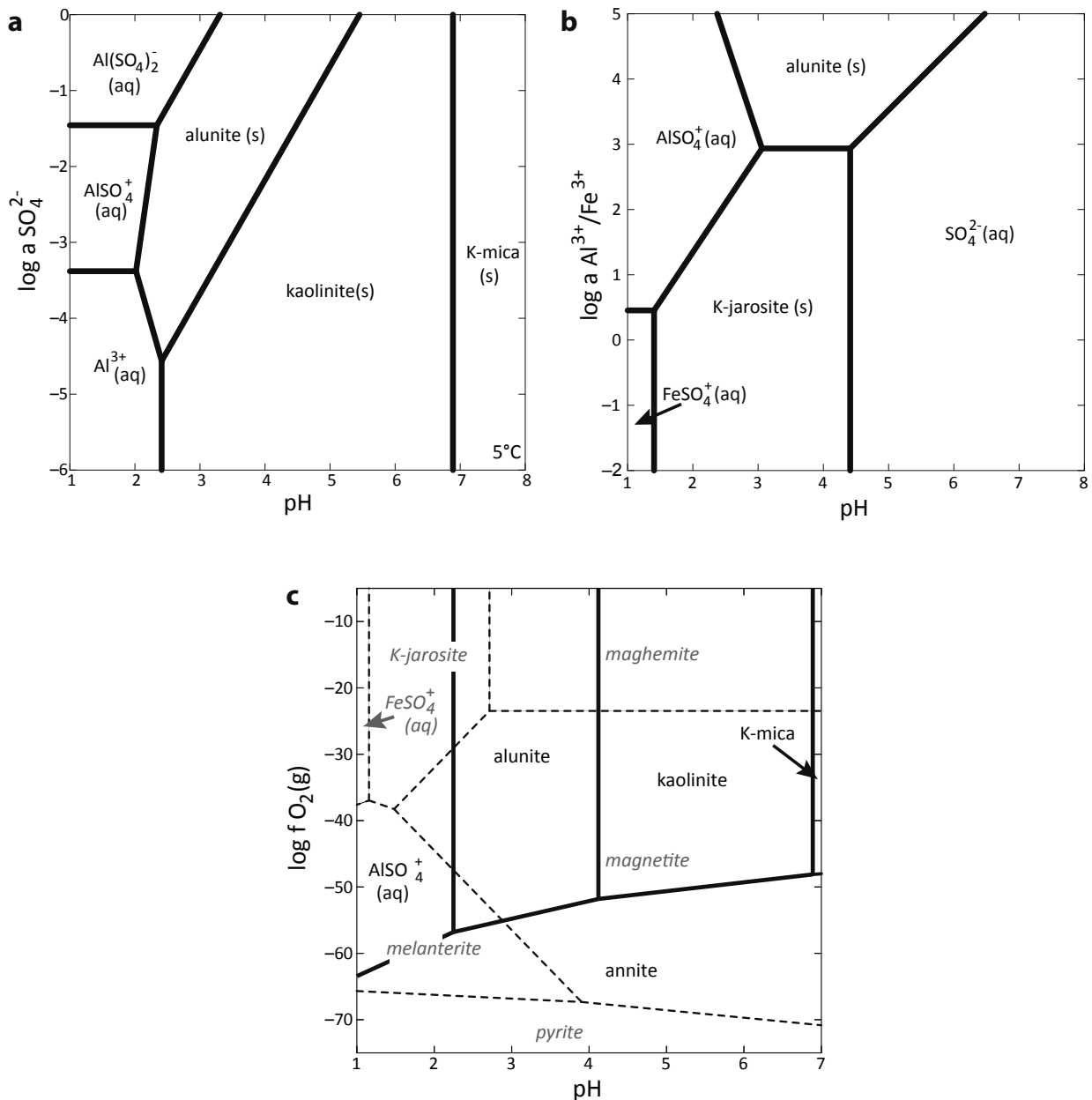


**FIGURE 8.** Predominance area diagrams to illustrate geochemical conditions favorable for alunite, kaolinite, and jarosite. Concentration of dissolved species and coexisting solid phases were based on simulated reaction of terrestrial volcanic gas compositions (Symonds et al. 2004) with martian basaltic composition (Poulet et al. 2009). **(a)** Plot of Al phases as a function of pH and sulfate activity. Alunite is favored at pH lower than kaolinite and with increasing sulfate activity. [Diagram calculated at:  $T = 5^\circ\text{C}$ ,  $P = 0.5$  bars,  $a_{\text{Mg}^{2+}} = 10^{-3}$ ,  $a_{\text{K}^+} = 10^{-3}$ ,  $a_{\text{Ca}^{2+}} = 10^{-3}$ ; kaolinite,  $\text{SiO}_2(\text{am})$  and  $\text{Fe}(\text{OH})_3(\text{am})$  have  $a = 1$ ; pyrophyllite, jurbanite, and laumontite are suppressed]. **(b)** Plot of sulfate phases as a function of pH and the ratio of  $\text{Al}^{3+}/\text{Fe}^{3+}$ , which must be high to favor alunite. [ $T = 5^\circ\text{C}$ ,  $P = 0.5$  bars,  $a_{\text{Mg}^{2+}} = 10^{-3}$ ,  $a_{\text{K}^+} = 10^{-5}$ ,  $a_{\text{SO}_4^{2-}} = 10^{-2}$ ,  $a_{\text{Ca}^{2+}} = 10^{-3}$ ;  $\text{SiO}_2(\text{am})$  and  $\text{Fe}(\text{OH})_3$  have  $a = 1$ ; jurbanite and basaluminite are suppressed.] **(c)** Superimposed predominance diagrams for Fe and Al phases as a function of pH and  $f_{\text{O}_2}$ . [ $T = 5^\circ\text{C}$ ,  $P = 0.5$  bars,  $a_{\text{Mg}^{2+}} = 10^{-3}$ ,  $a_{\text{K}^+} = 10^{-5}$ ,  $a_{\text{SO}_4^{2-}} = 10^{-2}$ ,  $a_{\text{Ca}^{2+}} = 10^{-3}$ ;  $\text{SiO}_2(\text{am})$ ,  $\text{Fe}(\text{OH})_3(\text{am})$ , and kaolinite have  $a = 1$ ; jurbanite, laumontite, pyrophyllite, goethite, and hematite are suppressed.] Diagrams calculated using Geochemist's Workbench v.8.0 using the Wateq4 database.

Cross crater basin and, perhaps, nearby Columbus crater and the plateaus between.

The acid aerosol mechanism may contribute to explaining regional Al-phyllsilicate formation by regional intensification of weathering (e.g., Wray et al. 2011; Ehlmann and Edwards

2014; Carter et al. 2015), but it does not explain the particular localized concentration of alunite in Cross crater. Iron sulfide dissolution or iron oxidation mechanisms likely provide a source of acidity elsewhere on Mars, but do not alone explain alunite formation here because of the paucity of Fe-bearing altera-

tion phases, which are typical products of this process and are detected with remote sensing at many other martian localities. Mars is mostly comprised of basaltic rocks, and the paucity of Fe/Mg/Ca secondary minerals and dominance of aluminum minerals in Cross crater is atypical.

Mineralized, layered sediments along a contour roughly coincident with the mouth of an inlet valley suggest the past presence of a closed basin lake in Cross crater. Lake levels at 1500 m (maximum elevation of layered sediments with Al-phyllosilicates) or 1650 m (inflow channel elevation) would have resulted in lake volumes of approximately 1500 or 1900 km<sup>3</sup>, respectively, comparable to the volume of terrestrial Lake Ontario (1700 km<sup>3</sup>). Alternatively, successive episodic periods of sedimentation and fill may have produced the observed sediments via a series of shallow playa lakes or via weathering of airfall deposits. Acquisition of additional HiRISE stereo pairs—only two on the southern wall exist to date—would facilitate the search for shoreline terraces and correlation of bed levels as indicators of lake level.

A key question is the source and nature of any waters feeding the basin. Although the depression in which the Cross crater inflow channel is sourced does not constitute a well-bounded basin, the entire region lies just east of the Eridania drainage network (Irwin et al. 2004), thought to be fed at least partially by groundwater (Fassett and Head 2008). Moreover, Cross crater is located south of the Mangala Vallis outflow, a unique valley system on Mars, where a large outflow is sourced by a small fracture. An extensive groundwater system has been suggested for the eastern flank of Tharsis (Ghatan et al. 2005 and references therein) and may provide a source of waters for a paleo-Cross crater lake. Waters may have acquired acidity by exchange with sulfurous compounds in meteoric waters or via subsurface exchange with hydrothermal fluids, paleobrines, or iron sulfides. As modeled by Andrews-Hanna et al. (2010) and discussed in Wray et al. (2011), Cross and Columbus craters are expected to be sites of groundwater upwelling forming closed basin lakes and evaporate deposits.

However, that the most spectrally dominant alunite is geographically restricted to the southwestern portion of the crater in spite of exposure of sedimentary materials with Al phyllosilicates across the whole crater argues for a process that concentrates the alunite formation in that area. In a ~800 m crater-wide deep lake, one would not expect highly localized chemistry except in special circumstances. One possibility is the presence of localized, perhaps fault-controlled, conduits for sulfurous groundwaters to reach the surface that are geographically restricted to the southwest and result in fumarolic or hydrothermal spring deposits. A second possibility is the existence of multiple shallow lakes within the basin, one of which was in the southwest corner. Because the alunite is topographically higher than the silica-rich and kaolin-rich deposits, the former possibility may be more likely than the latter. Additionally, the alunite units are massive, rather than discretely layered. This may reflect their formation in the subsurface as upwelling H<sub>2</sub>S- or SO<sub>2</sub>-bearing steam or fluids cooled, generating H<sub>2</sub>SO<sub>4</sub> through disproportionation. Oxidation upon contacting the Mars atmosphere or fluids in communication with the Mars atmosphere would still further enhance sulfur speciation to SO<sub>4</sub><sup>2-</sup>. Finally,

a third inter-crater plateau alunite-bearing site was found for which a non-lake-mediated formation process is favored. There, alunite also occurs mixed with kaolinite group minerals within light-toned deposits underlying an eroded cap-rock, but these are not in a topographic low.

Thus, localized conduits for escape of steam or waters in contact with magmatic sources at depth is our favored hypothesis for the Cross crater alunite deposits. Numerous basins on Mars show evidence of volcanic resurfacing (Goudge et al. 2012b), and Cross crater is located on the western margin of the Tharsis system (Fig. 1), a possible location of dike formation and a location with numerous tectonic fractures, facilitating communication with the subsurface (Anderson et al. 2001). The mineralogy of the Cross crater deposits with alunite, Al-phyllosilicates, silica, and scattered Fe oxides and Fe sulfates is similar to that observed in some terrestrial magmatic systems. A flux of steam or waters from a magmatic hydrothermal system into a basin that episodically may have hosted shallow lakes appears to fit the overall deposit morphology and observed mineral assemblages.

In terrestrial settings, large alunite deposits are more typically associated with acid alteration of either felsic rocks (e.g., Bigham and Nordstrom 2000) or preexisting Al phyllosilicates (e.g., Altheide et al. 2010). In basaltic hydrothermal alteration systems, alunite is often a minor phase (Swayze et al. 2002; Guinness et al. 2007; Hynke et al. 2013; Marcucci et al. 2013). However, large-scale alteration to alunite and kaolinite assemblages mappable by VSWIR imaging spectroscopy is also occasionally observed, driven in part by the duration of magmatic activity at a particular locale (e.g., Berger et al. 2003; Swayze et al. 2014). Furthermore, the crystallinity of protolith materials can strongly influence weathering products. Weathering experiments by Tosca et al. (2004) showed formation of Al-sulfates from basaltic glass but not crystalline basalt of identical chemical composition. This is because Al in a glassy material is released into solution during congruent dissolution, whereas Al is typically retained in rock in a dissolution process involving crystalline feldspar. Thus, (1) high throughput of acidic waters, (2) poorly crystalline materials, and/or (3) more felsic precursors may—separately or in combination—be responsible for the unique Cross crater alunite.

Future work might include more detailed geochemical modeling of various potential fluid and sediment compositions to further constrain the geochemical setting. Multistep formation scenarios could be modeled with reaction-transport models and compared to the composition and distribution of observed deposit mineralogy. A key question is the fate of leached Fe, Ca, and Mg, thus explaining the differences between Cross crater and nearby Columbus crater with its polyhydrated sulfate, gypsum, and kieserite deposits. These salts are either absent in Cross crater (precipitation in the subsurface, brine transport out of Cross crater through highly permeable rocks?) or concealed in the basin center by the caprock. Furthermore, questions of the potential extent, depth, and longevity of a Cross crater lake may be resolvable with additional high-spatial resolution mineralogic and topographic data over unimaged regions in Cross crater. A key question is whether any paleolakes and magmatic hydrothermal systems facilitating alunite formation were contemporaneous.

## IMPLICATIONS

Cross crater hosts the largest-scale alunite deposit discovered to date on Mars. It is associated with basin-ringing, layered kaolin-bearing sediments as well as hydrated silica or montmorillonite in polygonally fractured sediments within local topographic lows. Evidence for low-pH aqueous activity on Mars has been previously provided by ferric sulfates, including jarosite, formed at  $\text{pH} < 4$ . The discovery of alunite adds to the continuum of low-pH martian environments with a distinctly different local geochemistry resulting in relatively iron- (and magnesium- and calcium-) poor assemblages of phyllosilicates and sulfates. Along with the smaller deposits in nearby Columbus crater and on the plateau in between, Cross crater's alunite deposits are indicative of regional conditions. Prevalent alunite and accompanying Al phyllosilicates require acidity and (1) locally high volumes of sulfurous groundwaters with  $\text{H}_2\text{S}$  or  $\text{SO}_2$  and high water throughput during alteration; (2) atypically glassy and/or felsic basin-filling materials, more susceptible to dissolution and mobilization of aluminum; or a combination of these. Cross crater, with its advanced argillic alteration, including alunite precipitates, thus represents a new type of ancient martian aqueous environment.

Of the four mechanisms considered to produce the observed mineralogy and geomorphology—magmatic hydrothermal waters, massive sulfide weathering, brine-fed acid lakes, and deposition of atmospherically derived sulfurous aerosols—sulfurous magmatic hydrothermal waters and steam, rising through fractures, leaching local rocks, and then precipitating alunite upon fluid cooling and oxidation best explain the localized nature of the alunite deposits and their geomorphology. Evidence for regional groundwater upwelling, volcanism, and faulting as well as mineral assemblages similar to terrestrial magmatic hydrothermal environments are consistent with this scenario. Cross crater may have also episodically hosted a shallow lake in which the more widespread kaolin- and silica/montmorillonite-bearing sediments were deposited.

## ACKNOWLEDGMENTS

Many thanks to the science operations teams of CRISM, HiRISE, and CTX for their efforts in collecting this data set. Thanks to R. Rye for key discussions on mineralogy, C. Fassett for developing a program to access MOLA point shot data, T. Goudge for helpful discussions of martian impact crater volcanism and lacustrine deposits, P. Schultz for discussion of crater morphology and west Tharsis regional hydrology, J. Crowley for providing samples of lacustrine alunite, N. Pearson for research on prevailing wind directions, and S. Mattson for preparation of the Cross crater HiRISE DEM. Portions of this work were funded by investigator grants to the NASA MRO CRISM science team and participating scientists. Any use of trade, firm, or product names in this publication is for descriptive purposes only and does not imply endorsement by the U.S. Government.

## REFERENCES CITED

- Altheide, T.S., Chevrier, V.F., and Noe Dobrea, E. (2010) Mineralogical characterization of acid weathered phyllosilicates with implications for secondary martian deposits. *Geochimica et Cosmochimica Acta*, 74, 6232–6248.
- Anderson, R.C., Dohm, J.M., Golombek, M.P., Haldemann, A.F.C., Franklin, B.J., Tanaka, K.L., Lias, J., and Peer, B. (2001) Primary centers and secondary concentrations of tectonic activity through time in the western hemisphere of Mars. *Journal of Geophysical Research*, 106, 20,563–520,585, doi:10.1029/2000JE001278.
- Andrews-Hanna, J.C., Zuber, M.T., Arvidson, R.E., and Wiseman, S.M. (2010) Early Mars hydrology: Meridiani playa deposits and the sedimentary record of Arabia Terra. *Journal of Geophysical Research*, 115, E06002, doi:10.1029/2009JE003485.
- Ansan, V., et al. (2011) Stratigraphy, mineralogy, and origin of layered deposits inside Terby crater, Mars. *Icarus*, 211, 273–304, doi:10.1016/j.icarus.2010.09.011.
- Arvidson, R.E., et al. (2006) Nature and origin of the hematite-bearing plains of Terra Meridiani based on analyses of orbital and Mars Exploration rover data sets. *Journal of Geophysical Research*, 111, E12S08, doi:10.1029/2006JE002728.
- Benison, K.C., and Bowen, B.B. (2015) The evolution of end-member continental waters: The origin of acidity in southern Western Australia. *GSA Today*, 25(6), 4–10.
- Benison, K.C., Bowen, B.B., Oboh-Ikuenobe, F.E., Jagniecki, E.A., LaClair, D.A., Story, S.L., Mormile, M.R., and Hong, B. (2007) Sedimentary processes and products of ephemeral acid saline lakes in southern Western Australia. *Journal of Sedimentary Research*, 77, 366–388.
- Berger, B.R., King, T.V.V., Morath, L.C., and Phillips, J.D. (2003) Utility of high-altitude infrared spectral data in mineral exploration: Application to northern Patagonia Mountains, Arizona. *Economic Geology*, 98, 1003–1018.
- Bibring, J.-P., et al. (2005) Mars surface diversity as revealed by the OMEGA/Mars Express observations. *Science*, 307, 1576–1581, doi:10.1126/science.1108806.
- Bibring, J.-P., et al. (2006) Global mineralogical and aqueous Mars history derived from OMEGA/Mars Express data. *Science*, 312, 400–404, doi:10.1126/science.1122659.
- Bibring, J.-P., et al. (2007) Coupled ferric oxides and sulfates on the Martian surface. *Science*, 317, 1206–1210, doi:10.1126/science.1144174.
- Bigham, J.M., Nordstrom, D.K. (2000) Iron and aluminum hydroxysulfates from acid sulfate waters. *Reviews in Mineralogy and Geochemistry*, 40, 351–403.
- Bishop, J.L., and Murad, E. (2005) The visible and infrared spectral properties of jarosite and alunite. *American Mineralogist*, 90, 1100–1107.
- Bishop, J., Madejova, J., Komadel, P., and Froeschl, H. (2002a) The influence of structural Fe, Al, and Mg on the infrared OH bands in spectra of dioctahedral smectites. *Clay Minerals*, 37, 607–616, doi:10.1180/0009855023740063.
- Bishop, J.L., Murad, E., and Dyar, M.D. (2002b) The influence of octahedral and tetrahedral cation substitution on the structure of smectites and serpentines as observed through infrared spectroscopy. *Clay Minerals*, 37, 617–628, doi:10.1180/0009855023740064.
- Bishop, J.L., Lane, M.D., Dyar, M.D., and Brown, A.J. (2008) Reflectance and emission spectroscopy of four groups of phyllosilicates: Smectites, kaolinite-serpentines, chlorites, and micas. *Clay Minerals*, 43, 35–54, doi:10.1180/claymin.2008.043.1.03.
- Bishop, J.L., et al. (2009) Mineralogy of Juventae Chasma: Sulfates in the light-toned mounds, mafic minerals in the bedrock, and hydrated silica and hydroxylated ferric sulfate on the plateau. *Journal of Geophysical Research*, 114, E00D09, doi:10.1029/2009JE003352.
- Bowen, B.B., and Benison, K.C. (2009) Geochemical characteristics of naturally acid and alkaline saline lakes in southern Western Australia. *Applied Geochemistry*, 24, 268–284, doi:10.1016/j.apgeochem.2008.11.013.
- Bowen, B.B., Benison, K.C., and Story, S. (2012) Early diagenesis by modern acid brines in Western Australia and implications for the history of sedimentary modification on Mars. In J. Grotzinger and R. Milliken, Eds., *Mars Sedimentology*, 102, p. 229–252. Society for Sedimentary Geology Special Publication.
- Bullock, M.A., and Moore, J.M. (2007) Atmospheric conditions on early Mars and the missing layered carbonates. *Geophysical Research Letters*, 34, L19201, doi:10.1029/2007GL030688.
- Carr, M.H. (1996) *Water on Mars*, 248 pp. Oxford University Press, U.K.
- Carter, J., Poulet, F., Bibring, J.-P., Mangold, N., and Murchie, S. (2013) Hydrous minerals on Mars as seen by the CRISM and OMEGA imaging spectrometers: Updated global view. *Journal of Geophysical Research Planets*, 118, doi:10.1029/2012JE004145.
- Carter, J., Loizeau, D., Mangold, N., Poulet, F., and Bibring, J.-P. (2015) Widespread surface weathering on early Mars: A case for a warmer and wetter climate. *Icarus*, 248, 373–382.
- Christensen, P.R., et al. (2001) Mars Global Surveyor Thermal Emission Spectrometer experiment: Investigation description and surface science results. *Journal of Geophysical Research*, 106(E10), 23,823–823,871, doi:10.1029/2000JE001370.
- Christensen, P.R., et al. (2004) The Thermal Emission Imaging System (THEMIS) for the Mars 2001 Odyssey mission. *Space Science Reviews*, 110, 85–130, doi:10.1023/B:SPAC.0000021008.16305.94.
- Clark, R.N., King, T.V.V., Klejwa, M., Swayze, G.A., and Vergo, N. (1990) High spectral resolution reflectance spectroscopy of minerals. *Journal of Geophysical Research*, 95, 12,653–12,680, doi:10.1029/JB095iB08p12653.
- Clark, R.N., Swayze, G.A., Livo, K.E., Kokaly, R.F., Sutley, S.J., Dalton, J.B., McDougal, R.R., and Gent, C.A. (2003) Imaging spectroscopy: Earth and planetary remote sensing with the USGS Tetracorder and Expert Systems. *Journal of Geophysical Research*, 108, 5131, doi:10.1029/2002JE001847, 44 p.
- Clark, R.N., Swayze, G.A., Wise, R., Livo, E., Hoefen, T., Kokaly, R., and Sutley, S.J. (2007) USGS digital spectral library splib06a: U.S. Geological Survey, Data Series 231, <http://speclab.cr.usgs.gov/spectral-lib.html>.
- Dehouck, E., Chevrier, V., Gaudin, A., Mangold, N., Mathe, P.-E., and Rochette, P. (2012) Evaluating the role of sulfide-weathering in the formation of sulfates or carbonates on Mars. *Geochimica et Cosmochimica Acta*, 90, 47–63.
- Edwards, C.S., Nowicki, K.J., Christensen, P.R., Hill, J., Gorelick, N., and Murray, K. (2011) Mosaicking of global planetary image datasets: 1. Techniques

- and data processing for Thermal Emission Imaging System (THEMIS) multi-spectral data. *Journal of Geophysical Research*, 116, E10008, doi:10.1029/2010JE003755.
- Ehlmann, B.L. and Edwards, C.S. (2014) Mineralogy of the Martian Surface. *Annual Reviews of Earth and Planetary Sciences*, 42, doi: 10.1146/annurev-earth-060313-055024.
- Ehlmann, B.L., and Mustard, J.F. (2012) An in-situ record of major environmental transitions on early Mars at Northeast Syrtis Major. *Geophysical Research Letters*, 39, L11202, doi:10.1029/2012GL051594.
- Ehlmann, B.L., et al. (2008) Orbital identification of carbonate-bearing rocks on Mars. *Science*, 322, 1828–1832.
- Ehlmann, B.L., et al. (2009) Identification of hydrated silicate minerals on Mars using MRO-CRISM: Geologic context near Nili Fossae and implications for aqueous alteration. *Journal of Geophysical Research*, 114, E00D08, doi:10.1029/2009JE003339.
- Farrand, W.H., Glotch, T.D., Rice, J.W. Jr., Hurowitz, J.A., and Swayze, G.A. (2009) Discovery of jarosite within the Mawrth Vallis region of Mars: Implications for the geologic history of the region. *Icarus*, 204, 478–488.
- Farrand, W.H., Glotch, T.D., and Horgan, B. (2014) Detection of copiapite in the northern Mawrth Vallis region of Mars: Evidence of acid sulfate alteration. *Icarus*, 241, 346–357.
- Fassett, C.I., and Head, J.W., III (2008) Valley network-fed, open-basin lakes on Mars: Distribution and implications for Noachian surface and subsurface hydrology. *Icarus*, 198, 37–56.
- Ferguson, R.L. et al. (2006) High-resolution thermal inertia derived from the Thermal Emission Imaging System (THEMIS): Thermal model and applications. *Journal of Geophysical Research*, 111, E12004, doi:10.1029/2006JE002735.
- Fernández-Remolar, D., Rodríguez, N., Gómez, F., and Amils, R. (2003) The geological record of an acidic environment driven by iron hydrochemistry: The Tinto River system. *Journal of Geophysical Research*, 108, doi:10.1029/2002JE001918.
- Fernández-Remolar, D.C., Morris, R.V., Gruener, J.E., Amils, R., and Knoll, A.H. (2005) The Río Tinto basin, Spain: Mineralogy, sedimentary geobiology, and implications for interpretation of outcrop rocks at Meridiani Planum, Mars. *Earth and Planetary Science Letters*, 240, 149–167.
- Fernández-Remolar, D.C., Prieto-Ballesteros, O., Gómez-Ortiz, D., Fernández-Sampedro, M., Sarrazin, P., Gailhanou, M., and Amils, R. (2011) Río Tinto sedimentary mineral assemblages: A terrestrial perspective that suggests some formation pathways of phyllosilicates on Mars. *Icarus*, 211, 114–138, doi:10.1016/j.icarus.2010.09.008.
- Gaillard, F., Michalski, J., Berger, G., McLennan, S.M., and Scaillot, B. (2013) Geochemical reservoirs and timing of sulfur cycling. *Space Science Reviews*, 174, 251–300.
- Gendrin, A., et al. (2005) Sulfates in Martian layered terrains: The OMEGA/Mars Express view. *Science*, 307, 1587–1591, doi:10.1126/science.1109087.
- Ghatan, G.J., Head, J.W. III, and Wilson, L. (2005) Mangala Valles, Mars: Assessment of early stages of flooding and downstream flood evolution. *Earth, Moon, and Planets*, 96, 1–57.
- Gondet, B., Bibring, J.-P., Langevin, Y., Poulet, F., and Gendrin, A. (2006) First detection of Al-rich phyllosilicate on Mars from OMEGA-Mex. *Geophysical Research Abstracts*, 8, 03691, European Geosciences Union, 1607-7962/gra/EGU06-A-03691.
- Gouge, T.A., Head, J.W., Mustard, J.F., and Fassett, C.I. (2012a) An analysis of open-basin lake deposits on Mars: Evidence for the nature of associated lacustrine deposits and post-lacustrine modification processes. *Icarus*, 219, 211–229.
- Gouge, T.A., Mustard, J.F., Head, J.W., and Fassett, C.I. (2012b) Constraints on the history of open-basin lakes on Mars from the composition and timing of volcanic resurfacing. *Journal of Geophysical Research*, 117, E00J21, doi:10.1029/2012JE004115.
- Gouge, T.A., Aureli, K.L., Head, J.W., Fassett, C.I., and Mustard, J.F. (2015) Classification and analysis of candidate impact crater-hosted closed-basin lakes on Mars. *Icarus*, 260, 346–367.
- Guinness, E.A., Arvidson, R.E., Jolliff, B.L., Seelos, K.D., Seelos, F.P., Ming, D.W., Morris, R.V., and Graff, T.G. (2007) Hyperspectral reflectance mapping of cinder cones at the summit of Mauna Kea and implications for equivalent observations on Mars. *Journal of Geophysical Research*, 112, E08S11, doi:10.1029/2006JE002822.
- Hunt, G.R. (1977) Spectral signatures of particulate minerals, in the visible and near-infrared. *Geophysics*, 42, 501–513.
- Hunt, G.R., Salisbury, J.W., and Lenhoff, C.J. (1971) Visible and near-infrared spectra of minerals and rocks: IV. Sulphides and sulphates. *Modern Geology*, 3, 1–14.
- Hurowitz, J.A. and McLennan, S.M. (2007) A 3.5 Ga record of waterlimited, acidic weathering conditions on Mars. *Earth and Planetary Science Letters*, 260, 432–443, doi:10.1016/j.epsl.2007.05.043.
- Hurowitz, J.A., Fischer, W.W., Tosca, N.J., and Milliken, R.E. (2010) Origin of acidic surface waters and the evolution of atmospheric chemistry on early Mars. *Nature Geoscience*, 3, 323–326.
- Hynek, B.M., McCollom, T.M., Marcucci, E.C., Brugman, K., and Rogers, K.L. (2013) Assessment of environmental controls on acid-sulfate alteration at active volcanoes in Nicaragua: Applications to relic hydrothermal systems on Mars. *Journal of Geophysical Research Planets*, 118, 2083–2104, doi:10.1002/jgre.20140.
- Irwin, R.P., III, Howard, A.D., and Maxwell, T.A. (2004) Geomorphology of Ma'adim Vallis, Mars, and associated paleolake basins. *Journal of Geophysical Research*, 109, E12009, doi:10.1029/2004JE002287.
- John, D.A., Sisson, T.W., Breit, G.N., Rye, R.O., and Vallance, J.W. (2008) Characteristics, extent and origin of hydrothermal alteration at Mount Rainier Volcano, Cascades Arc, USA: Implications for debris-flow hazards and mineral deposits. *Journal of Volcanology and Geothermal Research*, 175, 289–314.
- Klingelhöfer, G., et al. (2004) Jarosite and hematite at Meridiani Planum from Opportunity's Mössbauer spectrometer. *Science*, 306, 1740–1745, doi:10.1126/science.1104653.
- Lichtenberg, K.A., et al. (2010) Stratigraphy of hydrated sulfates in the sedimentary deposits of Aram Chaos, Mars. *Journal of Geophysical Research*, 115, E00D17, doi:10.1029/2009JE003353.
- Long, D.T., Fegan, N.E., McKee, J.D., Lyons, W.B., Hines, M.E., and Macumber, P.G. (1992) Formation of alunite, jarosite and hydrous iron oxides in a hypersaline system: Lake Tyrell, Victoria, Australia. *Chemical Geology*, 96, 183–202.
- Malin, M.C., et al. (2007), Context Camera Investigation on board the Mars Reconnaissance Orbiter. *Journal of Geophysical Research*, 112, E05S04, doi:10.1029/2006JE002808.
- Marcucci, E.C., Hynek, B.M., Kierein-Young, K.S., and Rogers, K.L. (2013) Visible-near infrared reflectance spectroscopy of volcanic acid-sulfate alteration in Nicaragua: Analogs for early Mars. *Journal of Geophysical Research*, 118, 2213–2233, DOI:10.1002/jgre.20159.
- Mas, G.R., Mas, L.C., and Bengochea, L. (1996) Hydrothermal surface alteration in the Copahue geothermal field (Argentina). *Proceedings, 21st Workshop on Geothermal Reservoir Engineering*, Stanford University, Palo Alto California, January 22–24, SGP-TR-151.
- Massé, M., Le Mouélic, S., Bourgeois, O., Combe, J.-P., Le Deit, L., Sotin, C., Bibring, J.-P., Gondet, B., and Langevin, Y. (2008) Mineralogical composition, structure, morphology, and geological history of Aram Chaos crater fill on Mars derived from OMEGA Mars Express data. *Journal of Geophysical Research*, 113, E12006, doi:10.1029/2008JE003131.
- McArthur, J.M., Turner, J.V., Lyons, W.B., Osborn, A.O., and Thirwall, M.F. (1991) Hydrochemistry on the Yilgarn Block, Western Australia: Ferrollysis and mineralisation in acidic brines. *Geochimica et Cosmochimica Acta*, 55, 1273–1288, doi:10.1016/0016-7037(91)90306-P.
- McCollom, T.M., Ehlmann, B.L., Wang, A., Hynek, B.M., Moskowitz, B., and Berquo, T.S. (2014) Detection of iron substitution in natroalunite-natrojarosite solid solutions and potential implications for Mars. *American Mineralogist*, 99, 948–964.
- McEwen, A.S., et al. (2007) Mars Reconnaissance Orbiter's High Resolution Imaging Science Experiment (HiRISE). *Journal of Geophysical Research*, 112, E05S02, doi:10.1029/2005JE002605.
- Michalski, J.R., Cuadros, J., Niles, P.B., Parnell, J., Rogers, A.D., and Wright, S.P. (2013) Groundwater activity on Mars and implications for a deep biosphere. *Nature Geoscience*, 6, 133–138.
- Milliken, R.E., et al. (2008) Opaline silica in young deposits on Mars. *Geology*, 36, 847–850, doi:10.1130/G24967A.1.
- Milliken, R.E., Grotzinger, J.P., and Thomson, B.J. (2010) Paleoclimate of Mars as captured by the stratigraphic record in Gale Crater. *Geophysical Research Letters*, 37, L04201, doi:10.1029/2009GL041870.
- Morris, R.V., et al. (2008) Iron mineralogy and aqueous alteration from Husband Hill through Home Plate at Gusev Crater, Mars: Results from the Mössbauer instrument on the Spirit Mars Exploration Rover. *Journal of Geophysical Research*, 113, E12S42, doi:10.1029/2008JE003201.
- Murchie, S.L., et al. (2007) Compact Reconnaissance Imaging Spectrometer for Mars (CRISM) on Mars Reconnaissance Orbiter (MRO). *Journal of Geophysical Research*, 112, E05S03, doi:10.1029/2006JE002682.
- Murchie, S.L., et al. (2009a) A synthesis of Martian aqueous mineralogy after one Mars year of observations from the Mars Reconnaissance Orbiter. *Journal of Geophysical Research*, 114, E00D06, doi:10.1029/2009JE003342.
- Murchie, S.L., et al. (2009b) Compact Reconnaissance Imaging Spectrometer investigation and data set from the Mars Reconnaissance Orbiter's primary science phase. *Journal of Geophysical Research*, 114, E00D07, doi:10.1029/2009JE003344.
- Murchie, S., et al. (2009c) Evidence for the origin of layered deposits in Candor Chasma, Mars, from mineral composition and hydrologic modelling. *Journal of Geophysical Research*, 114, E00D05, doi:10.1029/2009JE003343.
- Mustard, J.F., et al. (2008) Hydrated silicate minerals on Mars observed by the CRISM instrument on MRO. *Nature*, 454, 305–309, doi:10.1038/nature07097.
- Osterloo, M.M., Hamilton, V.E., Bandfield, J.L., Glotch, T.D., Baldrige, A.M., Christensen, P.R., Tornabene, L.L., and Anderson, F. (2008) Chloride-bearing materials in the southern highlands of Mars. *Science*, 319, 1651–1654, doi:10.1126/science.1150690.
- Osterloo, M.M., Anderson, F.S., Hamilton, V.E., and Hynek, B.M. (2010) Geologic

- context of proposed chloride-bearing materials on Mars. *Journal of Geophysical Research*, 115, E10012, doi:10.1029/2010JE003613.
- Pelkey, S.M., et al. (2007) CRISM multispectral summary products: Parameterizing mineral diversity on Mars from reflectance. *Journal of Geophysical Research*, 112, E08S14, doi:10.1029/2006JE002831.
- Poulet, F., Bibring, J.-P., Mustard, J.F., Gendrin, A., Mangold, N., Langevin, Y., Arvidson, R.E., Gondet, B., and Gomez, C. (2005) Phyllosilicates on Mars and implications for early Martian climate change. *Nature*, 438, 623–627, doi:10.1038/nature04274.
- Poulet, F., Arvidson, R.E., Gomez, C., Morris, R.V., Bibring, J.-P., Langevin, Y., Gondet, B., and Griffes, J. (2008) Mineralogy of Terra Meridiani and western Arabia Terra from OMEGA/MEx and implications for their formation. *Icarus*, 195, 106–130, doi:10.1016/j.icarus.2007.11.031.
- Roach, L.H., et al. (2010) Hydrated mineral stratigraphy of Ius Chasma, Valles Marineris. *Icarus*, 206(1), 253–268, doi:10.1016/j.icarus.2009.09.003.
- Ruesch, O., Poulet, F., Vincendon, M., Bibring, J.-P., Carter, J., Erkeling, G., Gondet, B., Hiesinger, H., Ody, A., and Reiss, D. (2012) Compositional investigation of the proposed chloride-bearing materials on Mars using near-infrared orbital data from OMEGA/MEx. *Journal of Geophysical Research*, 117, E00J13, doi:10.1029/2012JE004108.
- Rye, R.O., Bethke, P.M., and Wasserman, M.D. (1992) The stable isotope geochemistry of acid sulphate alteration. *Economic Geology*, 87, 225–262.
- Settle, M. (1979) Formation and deposition of volcanic sulfate aerosols on Mars. *Journal of Geophysical Research*, 84, 8343–8354.
- Smith, D.E. et al. (2001) Mars Orbiter Laser Altimeter: Experiment summary after the first year of global mapping of Mars. *Journal of Geophysical Research Planets*, 106, 23,689–23,722.
- Squyres, S.W., et al. (2004a) The Spirit Rover's Athena Science Investigation at Gusev Crater, Mars. *Science*, 305, 794–799.
- Squyres, S.W., et al. (2004b) In situ evidence for an ancient aqueous environment at Meridiani Planum, Mars. *Science*, 306, 1709–1714.
- Squyres, S.W., et al. (2008) Detection of silica-rich deposits on Mars. *Science*, 320, 1063–1067.
- Stoffregen, R.E., Alpers, C.N., and Jambor, J.L. (2000) Alunite-jarosite crystallography, thermodynamics, and geochemistry. In C.N. Alpers, J.L. Jambor, and D.K. Nordstrom, Eds., *Sulfate Minerals: Crystallography, Geochemistry, and Environmental Significance*, 40, 453–479. Reviews in Mineralogy, Mineralogical Society of America, Chantilly, Virginia.
- Story, S., Bowen, B.B., Benison, K.C., and Schulze, D.G. (2010) Authigenic phyllosilicates in modern acid saline lake sediments and implications for Mars. *Journal of Geophysical Research*, 115, E12012, doi:10.1029/2010JE003687.
- Swayze, G.A. (1997) The hydrothermal and structural history of the Cuprite mining district, southwestern Nevada: An integrated geological and geophysical approach, 399 pp. Ph.D. thesis, University of Colorado, Boulder.
- Swayze, G.A., et al. (2000) Using imaging spectroscopy to map acidic mine waste. *Environmental Science and Technology*, 34, 47–54.
- Swayze, G.A., Clark, R.N., Sutley, S.J., Gent, C.A., Rockwell, B.W., Blaney, D.L., Post, J.L., and Farm, B.P. (2002) Mineral mapping Mauna Kea and Mauna Loa Shield Volcanos on Hawaii using AVIRIS data and the USGS Tetracorder spectral identification system: Lessons applicable to the search for relict Martian hydrothermal systems. In R.O. Green, Ed., *Proceedings of the 11th JPL Airborne Earth Science Workshop*, Jet Propulsion Laboratory Publication 03-4, 373–387.
- Swayze, G.A., Desborough, G.A., Clark, R.N., Rye, R.O., Stoffregen, R.E., Smith, K.S., and Lowers, H.A. (2006) Detection of jarosite and alunite with hyperspectral imaging: prospects for determining their origin on Mars using orbital sensors in martian sulfates as recorders of atmospheric-fluid-rock interactions. Workshop on Martian Sulfates as Recorders of Atmospheric-Fluid-Rock Interactions, October 22–24, 2006 in Houston, Texas. Lunar and Planetary Institute Contribution No. 7072.
- Swayze, G.A., et al. (2007) Spectral evidence for hydrated volcanic and/or impact glass on Mars with MRO CRISM. In Seventh International Conference on Mars, July 9–13, Pasadena, California, Lunar and Planetary Institute, Contribution No. 3384.
- Swayze, G.A., et al. (2008) Discovery of the acid-sulfate mineral alunite in Terra Sirenum, Mars, using MRO CRISM: Possible evidence for acid-saline lacustrine deposits? *Eos Transactions of the American Geophysical Union* 89(53), Fall Meeting Supplement, abstract P44A-04.
- Swayze, G.A., Clark, R.N., Goetz, F.H., Livo, K.E., Breit, G.N., Kruse, F.A., Sutley, S.J., Snee, L.W., Lowers, H.A., Post, J.L., Stoffregen, R.E., and Ashley, R.P. (2014) Mapping advanced argillic alteration at Cuprite, Nevada using imaging spectroscopy. *Economic Geology*, 109, 1179–1221, doi:10.2113/econgeo.109.5.1179.
- Thollot, P., et al. (2012) Most Mars minerals in a nutshell: Various alteration phases formed in a single environment in Noctis Labyrinthus. *Journal of Geophysical Research*, 117, E00J06, doi:10.1029/2011JE004028.
- Tosca, N.J., McLennan, S.M., Lindsley, D.H., and Schoonen, M.A.A. (2004) Acid-sulfate weathering of synthetic Martian basalt: The acid fog model revisited. *Journal of Geophysical Research*, 109, E05003, doi:10.1029/2003JE002218.
- Vaniman, D.T., et al. (2014) Mineralogy of a mudstone on Mars. *Science*, 343, 6169, doi:10.1126/science.1243480.
- Varekamp, J.C. et al. (2009) Naturally acid waters from Copahue volcano, Argentina. *Applied Geochemistry*, 24, 208–220.
- Wang, A., et al. (2008) Light-toned salty soils and coexisting Si-rich species discovered by the Mars Exploration Rover Spirit in Columbia Hills. *Journal of Geophysical Research*, 113, E12S40, doi:10.1029/2008JE003126.
- Weitz, C.M., Milliken, R.E., Grant, J.A., McEwen, A.S., Williams, R.M.E., Bishop, J.L., and Thompson, B.J. (2010) Mars Reconnaissance Orbiter observations of light-toned layered deposits and associated fluvial landforms on the plateau adjacent to Valles Marineris. *Icarus*, doi:10.1016/j.icarus.2009.04.017.
- Weitz, C.M., et al. (2011) Diverse mineralogies in two troughs of Noctis Labyrinthus, Mars. *Geology*, 39, 899–902, doi:10.1130/G32045.1.
- Wray, J.J., et al. (2011) Columbus crater and other possible groundwater-fed paleolakes of Terra Sirenum, Mars. *Journal of Geophysical Research*, 116, E01001, doi:10.1029/2010JE003694.
- Zolotov, M.Y., and Mironenko, M.V. (2014) Massive sulfate deposits on Mars could be remobilized Noachian salts. 45th Lunar and Planetary Science Conference, March 17–21, The Woodlands, Texas, abstract 2876.

MANUSCRIPT RECEIVED OCTOBER 1, 2015

MANUSCRIPT ACCEPTED MARCH 9, 2016

MANUSCRIPT HANDLED BY WILLIAM FARRAND